The Modified Stalk Mechanism of Lamellar/Inverted Phase Transitions and Its Implications for Membrane Fusion

David P. Siegel
Chemistry Department, The Ohio State University, Columbus, Ohio 43210 USA

ABSTRACT A model of the energetics of lipid assemblies (Siegel. 1993. *Biophys. J.* 65:2124–2140) is used to predict the relative free energy of intermediates in the transitions between lamellar (L_α) inverted hexagonal (H_{II}), and inverted cubic (Q_{II}) phases. The model was previously used to generate the modified stalk theory of membrane fusion. The modified stalk theory proposes that the lowest energy structures to form between apposed membranes are the stalk and the transmonolayer contact (TMC), respectively. The first steps in the L_α/H_{II} and L_α/Q_{II} phase transitions are also intermembrane events: bilayers of the L_α phase must interact to form new topologies during these transitions. Hence the intermediates in these phase transitions should be similar to the intermediates in the modified stalk mechanism of fusion. The calculations here show that stalks and TMCs can mediate transitions between the L_α, Q_{II}, and H_{II} phases. These predictions are supported by studies of the mechanism of these transitions via time-resolved cryoelectron microscopy (Siegel et al. 1994. *Biophys. J.* 66:402–414; Siegel and Epand. 1997. *Biophys. J.* 73:3089–3111), whereas the predictions of previously proposed transition mechanisms are not. The model also predicts that Q_{II} phases should be thermodynamically stable in all thermotropic lipid systems. The profound hysteresis in L_α/Q_{II} transitions in some phospholipid systems may be due to lipid composition-dependent effects other than differences in lipid spontaneous curvature. The relevant composition-dependent properties are the Gaussian curvature modulus and the membrane rupture tension, which could change the stability of TMCs. TMC stability also influences the rate of membrane fusion of apposed bilayers, so these two properties may also affect the fusion rate in model membrane and biomembrane systems. One way proteins catalyze membrane fusion may be by making local changes in these lipid properties. Finally, although the model identifies stalks and TMCs as the lowest energy intermembrane intermediates in fusion and lamellar/inverted phase transitions, the stalk and TMC energies calculated by the present model are still large. This suggests that there are deficiencies in the current model for intermediates or intermediate energies. The possible nature of these deficiencies is discussed.

INTRODUCTION

Lamellar (L_α), inverted cubic (Q_{II}), and inverted hexagonal (H_{II}) phases have very different topologies. The transitions between these phases have to make substantial changes in topology. In particular, they must make or break extensive connections between lipid/water interfaces. In this respect, the transition mechanisms resemble the first steps in membrane fusion. Many researchers have speculated that the first intermediates in these two different processes, fusion and lamellar/inverted phase transitions, are similar. A structure known as a "stalk" has been proposed as the first intermediate to form in the process of membrane fusion (Markin et al., 1984; Chernomordik et al., 1985, 1987; Leikin et al., 1987; Kozlov et al., 1989; Siegel, 1993). The stalk hypothesis is fairly successful in rationalizing many observations concerning fusion in model and biomembrane systems (Chernomordik et al., 1995a; Siegel, 1993; Basáñez et al., 1998; see Chernomordik et al., 1995b, and Chernomordik and Zimmerberg, 1995 for reviews). It is therefore important to see if a phase transition mechanism based on stalk intermediates can also explain the observed dynamics of lamellar/inverted phase transitions.

Siegel (1993) developed a method for estimating the energies of hypothetical intermediate structures with respect to planar bilayers, which is an elaboration of the technique of Markin et al. (1984). The method is based on studies of the relative energies of lipids in lamellar and inverted phases by Gruner, Parsegian, Rand, and others (for reviews, see Gruner (1990), Lindblom and Rilfors (1989), Seddon (1990), and Tate et al. (1991)). Kozlov et al. (1994) have used a method with the same principal elements to reproduce a complex portion of the phase diagram of water/dioleoylphosphatidylethanolamine (DOPE). This demonstrates that the method yields fairly accurate results. Siegel (1993) used the method to propose a modification of the original stalk theory of membrane fusion.

Here the same method is used to find the lowest-energy sequence of intermediate structures capable of generating H_{II} and Q_{II} phases from an L_α phase. The calculations are made for the lipid DOPE, using the same bending elastic modulus and the same temperature-dependent H_{II} unit cell dimensions in excess water as Kozlov et al. (1994). The energies of the structures can be calculated as a function of temperature, so we can also estimate how the relative stability of the different structures changes with temperature.

Received for publication 26 January 1998 and in final form 15 September 1998.

Address reprint requests to Dr. David Paul Siegel, Chemistry Department, The Ohio State University, 120 West 18th Avenue, Columbus, OH 43210. Tel.: 614-688-4568; Fax: 614-292-1532; E-mail: dsiegel@chemistry.ohio-state.edu.

0006-3495/99/01/291/23 $2.00

The first intermediates to form during lamellar/inverted phase transitions should be the same as in the stalk theory (Markin et al., 1984). In the process of fusion, stalks were originally proposed to expand radially to form extensive areas of single-bilayer diaphragm between apposed liposomes (e.g., Markin et al., 1984). However, Siegel (1993) showed that, in lipid systems without apolar oils or alkanes, radial expansion should be limited, and stalks should expand radially into smaller structures known as hemifusion intermediates or transmonolayer contacts (TMCs). TMCs are critical intermediates in the fusion process, because they can decay into fusion pores. Here it is shown that TMCs should also play an important role in the lamellar (L_α)/inverted hexagonal (H_{II}) phase transition. TMCs can aggregate within the planes of apposed bilayers to form a structure that can elongate directly into a domain of H_{II} phase. In a recent study of the L_α/H_{II} transition mechanism via time-resolved cryo-transmission electron microscopy (TRC-TEM), Siegel and Epand (1997) presented evidence for the existence of this aggregate of TMCs. A transition mechanism based on TMCs is also more compatible with observations than mechanisms based either on inverted micellar intermediates (Siegel, 1986a) or on "conical LIPs" (Hui et al., 1983) for another reason. Hui et al. (1983) speculated that stalk-like intermediates could elongate directly into line defects, which are structures resembling part of an H_{II} phase unit cell. A similar structure was invoked by Siegel (1986a). Here it is shown that this process is not spontaneous.

It was proposed (Siegel, 1993) that individual TMCs can rupture to form fusion pores (also called interlamellar attachments or ILAs; Siegel, 1986a,b). ILAs are structural elements that assemble into Q_{II} phases (Siegel, 1986c; Siegel et al., 1989c; Frederik et al., 1991). Here it is shown that, as a lipid system is heated toward T_H, thermodynamically stable ILAs and Q_{II} phases should form. The Q_{II} phase should then form H_{II} phase at higher temperatures. This behavior is observed in many systems with thermotropic lamellar/inverted phase transitions.

It is clear that formation of ILAs and Q_{II} phases is very slow and hysteretic in some systems. Presumably, the rate of ILA formation from TMCs determines whether the L_α phase in a given system forms Q_{II} phases (by accumulation of many ILAs) or H_{II} phases (by accumulation of a large steady-state population of TMCs) on the experimental time scale. Composition-dependent factors other than the curvature elastic energy and interstice energies may affect the rate of fusion pore (ILA) formation from TMCs. Some of these factors, particularly the composition-dependent bilayer rupture tension, are discussed here. The results suggest an important new means by which low levels of particular lipids like lysolipids, or certain types of peptides, could substantially enhance the rate of fusion in model membranes and biomembranes. A summary of some of the results of this theoretical analysis has been presented elsewhere (Siegel and Epand, 1997).

THEORETICAL RESULTS

Principles of the method for calculating intermediate energies

The energies of the intermediates are treated as the sum of the curvature elastic energies of the lipid monolayers and the formation energies of hydrophobic interstices within the structures. Details are given in Siegel (1993) and Appendix 1. Briefly, the curvature elastic energy (G_c) of a lipid monolayer is calculated by the method of Helfrich (1973): the energy is of the form

$$G_c = -(k_m/2)\int_A [C_1 + C_2 - C_0]^2 dA,$$

where k_m and C_0 are lipid composition-dependent properties that can be measured by appropriate x-ray diffraction experiments, C_1 and C_2 are the principal radii of curvature of the monolayer, and the integral is taken over the area of the monolayer surface. The curvatures and area are evaluated at a defined plane within the thickness of the monolayer. Hydrophobic interstices are found in the H_{II} phase and have a positive free energy of formation. The energy can be calculated from results of structural studies of these phases (Siegel, 1993).

The first intermediates to form during bilayer/nonbilayer transitions are probably stalks, which transform into TMCs

It was previously proposed that the first intermediate to form between two apposed membranes (Fig. 1 *A*) during membrane fusion is the stalk (Markin et al., 1984; Chernomordik et al., 1985, 1987; Leikin et al., 1987; Kozlov et al., 1989). The calculations of Siegel (1993) also support this view. Of the hypothetical intermembrane intermediates that have been proposed so far, stalks have the lowest energy. A stalk is depicted in Fig. 1 *B*. The structure is cylindrically symmetrical about the dashed vertical axis and has a shape like a thread spool or the center of an hourglass.

A stalk can either revert to the original bilayer structure or form a trans monolayer contact (TMC), depicted in Fig. 1 *C*. The high-curvature region of the *cis* monolayer of the stalk expands radially, and the *trans* monolayers of the original bilayers dimple inward to contact each other in the center. This forms a bilayer diaphragm composed only of lipids originally found in the *trans* (nonapposed) monolayers of the two apposed bilayers. This diaphragm is surrounded by a linear hydrophobic interstice. The unfavorable energy of interstice creation prevents the bilayer diaphragm from growing in diameter by more than a nanometer or so. A TMC can greatly reduce its energy by diaphragm rupture, which produces an ILA (Fig. 1 *D*). An ILA is the same as a fusion pore, so formation of an ILA between two apposed liposomes corresponds to membrane fusion.

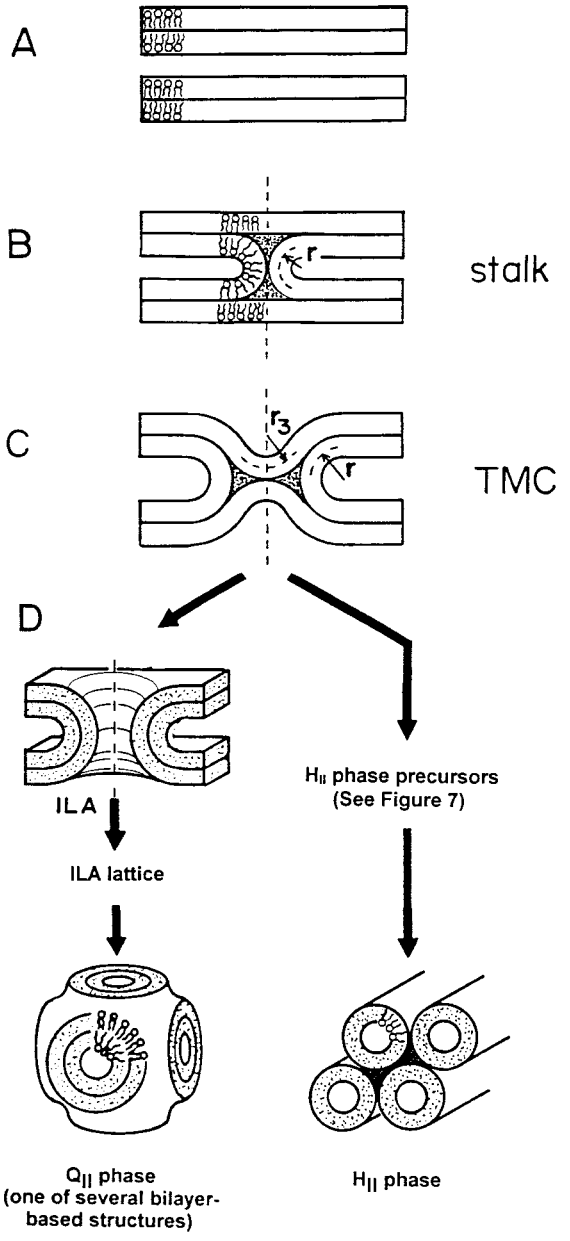

FIGURE 1 The modified stalk theory of membrane fusion and inverted phase. (*A*) Planar L_α phase bilayers. (*B*) Stalk. The stalk is cylindrically symmetrical about the dashed vertical axis. It is composed only of lipids in the apposed (*cis*) monolayers of the two bilayers. (*C*) *Trans* monolayer contact (TMC) or hemifusion intermediate. (*D*) TMCs can form two different types of structures. If the bilayer diaphragm in the middle of the TMC ruptures, it forms a fusion pore (also referred to as an interlamellar attachment or ILA). *Left*: A cross section through a perspective view of an ILA. If ILAs accumulate in sufficient numbers, they form ILA lattices, which can rearrange to form Q_{II} phase. *Right*: For systems close to the L_α/H_{II} phase boundary, TMCs can also aggregate to form H_{II} phase precursors, which will be discussed later (Fig. 7). In *C* and *D* the edges of lipid monolayers are stippled. Figure adapted from Siegel and Epand (1997).

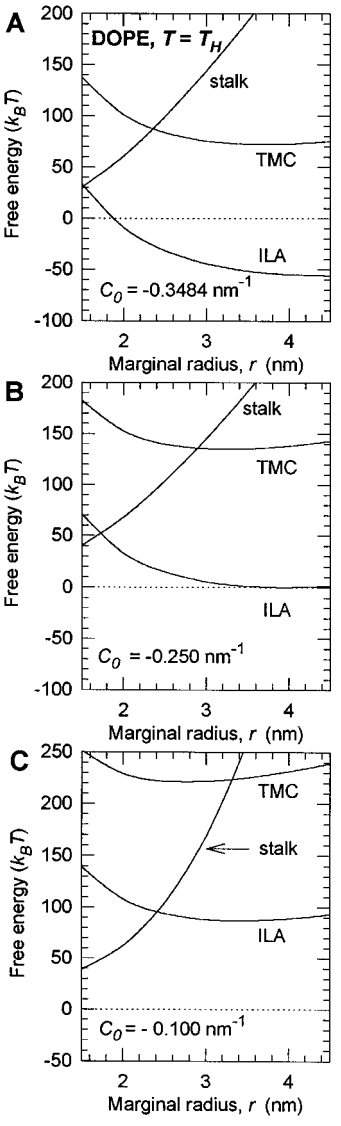

FIGURE 2 Plots of the free energy of stalks, TMCs, and ILAs as a function of marginal radius, *r*, for systems with different values of C_0. (*A*) $C_0 = -0.3484\ \text{nm}^{-1}$, corresponding to DOPE at $T = T_H$. (*B*) (*B*) $C_0 = -0.250\ \text{nm}^{-1}$. This corresponds to a mixture of DOPE/DOPC $\approx$ 3/2 mol/mol at around room temperature. (*C*) $C_0 = -0.100\ \text{nm}^{-1}$, corresponding roughly to pure DOPC at room temperature. Energies are in units of k_BT, where k_B is Boltzmann's constant and $T = 298$ K.

The energies of stalks, TMCs, and ILAs change as a function of size. In Fig. 2 *A*, the energies of these intermediates in dioleoylphosphatidylethanolamine (DOPE) are plotted as a function of *r*, the marginal radius of the original stalk, under conditions corresponding to $T = T_H$, with $\varepsilon = 0$. Stalks can always reduce their energy by shrinking (decreasing *r*). However, stalks that form with a large enough value of *r* will be able to spontaneously form a TMC. For comparison, similar plots are given for the energies of the intermediates in systems with $C_0 = -0.25$ and $-0.1\ \text{nm}^{-1}$ in Fig. 2, *B* and *C*. These values are the values expected for DOPE/DOPC $\approx$ 3/2 mol/mol, and pure DOPC; respectively. The energies of TMCs and ILAs increase with increasing C_0.

How might these intermediate structures mediate lamellar/inverted phase transitions? We wish to test whether

stalks, TMCs, and ILAs can generate H_{II} and Q_{II} phases from the L_α phase. Let us discuss the mechanism of the L_α/Q_{II} phase transition first, because it arises very naturally from the results already obvious in Fig. 2. Then we will return to the mechanism of the L_α/H_{II} phase transition, which is more subtle.

ILAs and inverted cubic phases are thermodynamically stable in a temperature interval around T_H

Previous work indicates that ILAs are Q_{II} phase precursors (Siegel, 1986c; Siegel et al., 1989c). Therefore, if the modified stalk theory generates large numbers of ILAs in systems in the appropriate temperature range, then it is capable of producing Q_{II} phase formation. Q_{II} phases should also be stable through at least part of the temperature interval in which ILAs are stable.

An important and obvious feature of the results in Fig. 2 is that ILAs are much more stable than planar bilayers at T_H. T_H is defined as the temperature at which the free energies of lipid in the L_α and H_{II} phases are equal. If formation of no other structure intervenes, this will be the temperature at which the L_α/H_{II} phase transition occurs. However, the model predicts that there should also be polymorphism (ILA and Q_{II} phase formation) in the vicinity of T_H. In fact, ILAs are predicted to be thermodynamically stable in general for a substantial temperature region around T_H.

We can estimate the temperature range for ILA stability by calculating the free energy of ILAs as a function of C_0. C_0 is a function of temperature. As T increases, C_0 decreases (becomes more negative). At some value of C_0, the free energy of the ILA will be the same as an equivalent area of planar L_α phase bilayer. This should correspond to the lowest temperature at which ILAs will form in significant numbers. The highest temperature for ILA formation will be the temperature where the free energy of the ILA equals the free energy of an equivalent amount of H_{II} phase lipid. Above that temperature, at equilibrium, H_{II} phase will form in preference to ILAs. The temperature dependence of C_0 has been obtained from the temperature dependence of the unit cell dimensions of the H_{II} phase (Tate and Gruner, 1989; Kozlov et al., 1994). It is convenient to express C_0 as its inverse, R_0. For small temperature intervals around $T = T_H$ (Kozlov et al., 1994),

$$\frac{d|R_0|}{dT} \approx -0.015 \text{ nm/K}. \quad (1)$$

In Fig. 2, it is obvious that the free energy of ILAs decreases (they become more stable) as the temperature increases toward T_H. However, it is also clear from Fig. 2 that the ILA energy at any given C_0 or T depends on the value of the marginal radius r. In fact, the equilibrium energy of an ILA is sensitive to both the marginal radius and the axial radius of the final ILA structure. To compute the energy of an ILA as a function of temperature, we need to know the equilibrium dimensions of an ILA as a function of C_0. We will attack this problem first and then return to the problem of determining the temperature range of ILA stability.

Equilibrium dimensions of ILAs

Once formed from a TMC, an ILA should be able to expand or contract to reach dimensions at which it is more stable. Chizmadzhev et al. (1995) have previously shown this for fusion pores, evaluating the curvature energy on a bilayer basis. Here, similar calculations are made, evaluating the curvature energy of the structure as the sum of the energies of both monolayers, which gives a more accurate account of the energy at small ILA dimensions and a more accurate account of the C_0 dependence of the energy. The energy of an isolated ILA is plotted as a function of size in Fig. 3 *A*, for the value of C_0 at $T = T_H - 10$ K. The radii are displayed as the values at the midplane of the bilayer surface of the ILA, to ease interpretation in terms of the

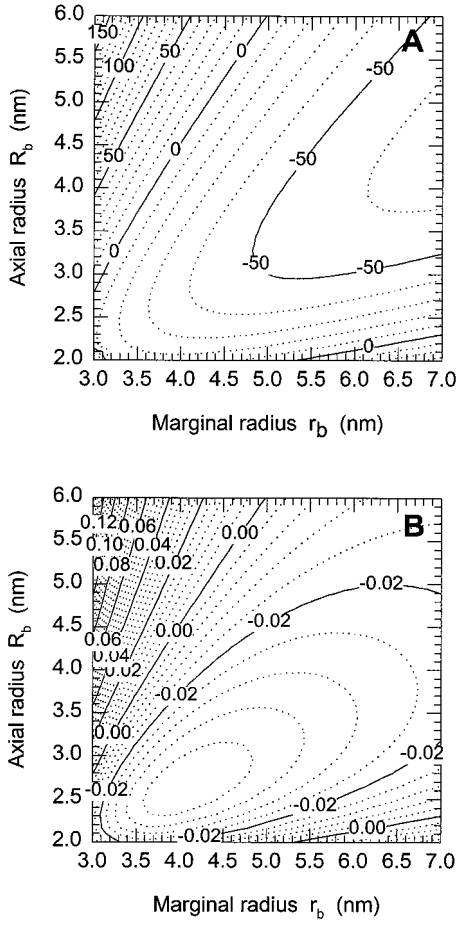

FIGURE 3 (*A*) The free energy of an ILA as a function of the marginal radius r_b and axial radius R_b, both evaluated at the bilayer midplane. $C_0 = -0.3311$ nm^{-1} (DOPE at $T = T_H - 10$ K). An ILA with small values of r_b and R_b will increase in size in both dimensions to lower the curvature energy (in k_BT). (*B*) The free energy per lipid molecule (k_BT/molecule) of an ILA as a function of r_b and R_b. There is a unique size that minimizes the energy per lipid ($r_b = 4.1$ nm and $R_b = 2.66$ nm).

overall dimensions of the ILA. The marginal radius r_b is the radius in the plane of the ILA axis, and R_b is the axial radius of the ILA. The lowest energy region is a trough that extends to the upper right of the diagram. An isolated ILA would expand to large values of r_b and R_b, although the slope of the surface in this trough is very small at large radii, and the rate of expansion would eventually become trivial. This dependence is qualitatively very similar to that described by Chizmadzhev et al. (1995). If an ILA can expand almost indefinitely, as Fig. 3 *A* implies, what other constraints will limit this expansion and determine the true energy?

The free energy of an individual ILA is lower than an equivalent area of planar bilayer, but the energy decreases more and more slowly as the ILA expands. Therefore the free energy of the system as a whole can be minimized by producing many ILAs with more modest dimensions. We calculate this area-minimized energy by dividing the total ILA energy by the area of bilayer in the ILA. The result is expressed as a free energy per lipid molecule, using the area per lipid molecule $a = 0.65$ nm^2 for DOPE (Kozlov et al., 1994). The area of bilayer in an ILA is

$$A = 2\pi^2 r_b(R_b + r_b) - 4\pi r_b^2. \quad (2)$$

The energy per lipid in an ILA is plotted in Fig. 3 *B*, for a C_0 value corresponding to $T = T_H - 10$ K. Note that now there is a minimum-energy dimension, although the minimum is rather broad. The most stable ILA at T_H has r_b and R_b values of ~4.1 and ~2.66 nm, respectively. If a bilayer is 4 nm thick, this corresponds to an ILA "waist" diameter of ~9 nm. The same procedure can be used to calculate the equilibrium dimensions of ILAs at any value of C_0.

The ILA dimensions calculated in this manner are in fairly good agreement with observations. The observed "waist" diameter of ILAs in similar systems varies across a wide range, as expected on the basis of the broad minima in Fig. 3 *B*, but is usually 12–15 nm (Siegel et al., 1989c; Frederik et al., 1991). This is somewhat larger than the predicted value. However, the only ILAs whose dimensions can be accurately measured via cryoelectron microscopy are those that are comparatively isolated (i.e., not in multilamellar arrays that are densely packed with ILAs, where superposition effects obscure the features of individual structures). Isolated ILAs are still free to expand to larger dimensions, as indicated in Fig. 3 *A*: they have not come up against the constraint of maximizing the number of ILAs per unit area. Thus they may be larger than the area-minimized dimensions calculated above.

The upper temperature limit of ILA stability

As the temperature, T, increases, the H_{II} phase should eventually become more stable than ILAs. To find this temperature, we need expressions for the free energies of lipid in the H_{II} phase as a function of T. The free energy per molecule of lipid in the H_{II} phase with respect to the L_α phase is given by (Siegel, 1993)

$$G_H(T) = \frac{ak_m}{2}[-1/r_H(T)^2 + 1/r_H(T_H)^2], \quad (3)$$

where the interstice energy has been expressed in terms of k_m and r_H (equation 4 of Siegel, 1993). $r_H(T)$ is the radius of the H_{II} phase monolayers as a function of T, $r_H(T_H)$ is the value of this radius at $T = T_H$, and a is the area per lipid molecule at the monolayer midplane. In this derivation, it is assumed that $r_H(T)$ is always equal to $-R_0(T)$, which appears to be an excellent approximation (Kozlov et al., 1994), and that a is constant throughout the relevant temperature regime. When the area-minimized energies of ILAs (obtained from plots like Fig. 3 *B*) and H_{II} phase (Eq. 3) are plotted as a function of C_0, the plots intersect at a value of C_0 corresponding to $T = T_H + 13$°C (Fig. 4).

The lower temperature limit for ILA stability

The lower temperature limit for ILA stability should be the temperature at which the free energy of ILA lipid is the same as an equivalent amount of L_α phase lipid. The free energy per lipid molecule in ILAs and H_{II} phase is plotted versus temperature in Fig. 4. These energies are referenced to the free energy of L_α phase lipid, which is defined as zero at all temperatures. The free energy of ILA lipid decreases asymptotically to that of L_α phase lipid as the temperature decreases. Therefore, it is difficult to make an accurate prediction of the lower temperature limit of ILA stability: the slope of the ILA energy versus temperature plot is small, and small imperfections in the model produce large differences in the estimated intersection temperature. For instance, at 70 degrees below T_H, the free energy per lipid molecule in an ILA is $0.011k_BT$ less than the free energy of L_α phase lipid. This difference is only halved by a further 30 degree reduction in temperature.

The true onset temperature is probably higher. TMCs are precursors to ILAs, and the free energy required to produce TMCs increases with decreasing temperature. TMCs may be too rare for there to be any significant rate of ILA production at very low temperatures (see below). Moreover, the calculation assumes that R_0 depends linearly on temperature (Eq. 1), and that the curvature elastic modulus k_m is independent of temperature. Both of these assumptions are unrealistic for such a large temperature range of 100 degrees. As T decreases, R_0 may increase faster than indicated by Eq. 1, and the bilayers probably become more rigidly planar as they approach the L_α/L_β phase transition temperature, T_c, where the acyl chains freeze. In fact, the T_c of DOPE is only 26 degrees below T_H (Marsh, 1990). Since gel phase bilayers are apt to have larger values of R_0, ILAs are not expected to form from gel phases. Therefore, our rough estimate for the onset temperature for ILA formation is that ILAs can start to appear at T_c but should become numerous only at higher temperatures. This is consistent

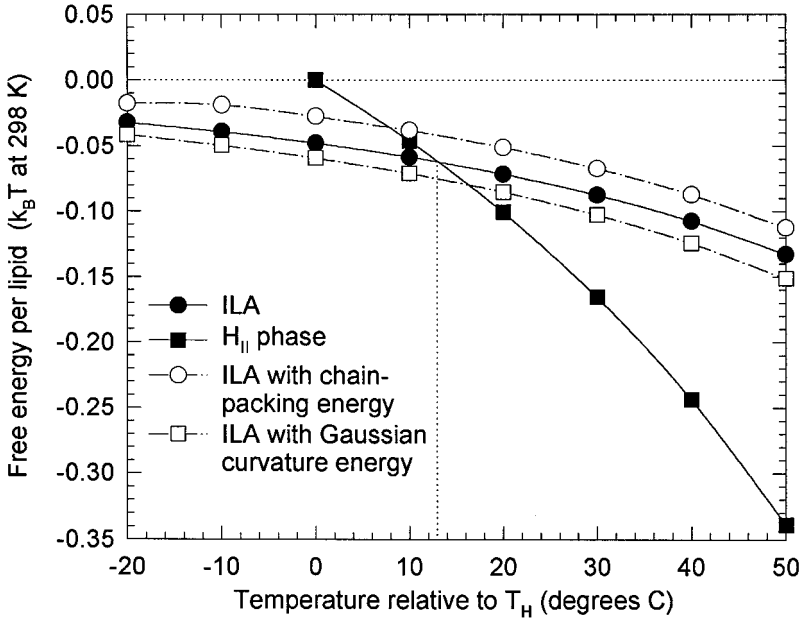

FIGURE 4 ILA and H_{II} phase energy as a function of temperature. Filled squares: H_{II} phase. Filled circles: ILA with only geometric mean curvature energy. The dotted vertical line indicates the temperature at which H_{II} phase becomes more stable than an array of ILAs. Circles: ILA with chain-packing energy included. Squares: ILA with Gaussian curvature energy included. See Appendix 2 for a discussion of the chain packing and Gaussian curvature energies.

with the observation by many authors (e.g., Cullis et al., 1978; Ellens et al., 1986, 1989) that ILAs formed at high temperature only revert to bilayer structure when the system is cooled to low temperatures (below T_c), and Q_{II} phases have recently been observed to transform directly to the gel phase at T_c (Tenchov et al., 1998). The effects of including Gaussian curvature and chain-packing energies on the temperature range of ILA stability are estimated in Appendix 2.

How well does the predicted temperature range of ILA stability agree with observed behavior?

Therefore, if we consider only the geometric mean curvature elastic energy of ILAs, the present model predicts that ILAs are stable in a temperature region extending from T_c to ~13 K above T_H. Q_{II} phases, which assemble from ILAs, should be stable through at least part of this temperature range. The possible mechanisms of transformation of ILA arrays into Q_{II} phase, and of Q_{II} phase into H_{II} phase, are discussed at the end of this Results section.

The range of ILA stability is predicted relative to the value of T_H, so one can determine how well the model predicts the temperature range of ILA stability only in systems in which the L_α/Q_{II} transition is so hysteretic that one can accurately measure T_H. T_H also has to be far enough above the ice point and far enough above the L_β/L_α phase transition for the onset of ILA formation to be easily observable. N-methylated DOPE (DOPE-Me) is a system that meets both of these requirements, because it has a T_c of −12.5°C (Gruner et al., 1988) and a T_H of 66°C (Ellens et al., 1989; Siegel et al., 1989a,c). DOPE-Me has H_{II} phase structural dimensions at T_H that are similar to those of DOPE and probably has a similar value of k_m, because of the similar structure of the acyl chains and headgroups. ILAs appear in DOPE-Me between 30 and 40 K below T_H, as observed by cryoelectron microscopy and ^{31}P NMR (Gagné et al., 1985; Ellens et al., 1989; Siegel et al., 1989a,c). ILAs must form in significant numbers to be visible by either technique, so it is possible that small numbers of ILAs form at even lower temperatures. For instance, 1 or 2% of the lipid in the system must exist as ILAs to be detected via ^{31}P NMR (Ellens et al., 1989). Siegel and Banschbach (1990) found that the Q_{II} phase in DOPE-Me is stable to ~6–13 K above T_H. ILAs, detected as an isotropic ^{31}P NMR resonance, are present at temperatures at least 14 K above T_H (Gagné et al., 1985). Therefore, the observed range of ILA stability is reasonably close to the predictions of this simple theory.

Do all thermotropic systems form the Q_{II} phase at lower temperatures than the H_{II} phase, as predicted?

Many thermotropic systems form Q_{II} phases in a temperature interval between L_α and H_{II} phases, as required by the present model. Examples include the monoglycerides (e.g., Caffrey, 1987; Briggs and Caffrey, 1994) and branched-chain phosphatidylcholines (Lewis et al., 1994). However, there are also many systems in which L_α/Q_{II} transitions are either very slow and hysteretic, or absent. Principal examples are pure phosphatidylethanolamines and some N-alkylated phosphatidylethanolamines. Q_{II} phases form in DOPE at around T_H, but they must be induced by temperature-cycling across T_H (Shyamsunder et al., 1988). While DOPE-Me spontaneously forms Q_{II} phases in this interval, the transition is very slow (Gruner et al., 1988; Siegel and Banschbach, 1990). Tenchov et al. (1998) recently reported formation of Q_{II} phases by temperature cycling in four PEs and one PE derivative. Other N-alkylated phosphatidylethanolamines show signs of the same behavior (Leventis et

al., 1991). Finally, although many glycolipids readily form Q_{II} phases (e.g., Mannock et al., 1992), others only show signs of hysteretic Q_{II} phase formation (Mannock et al., 1994).

These observations imply that Q_{II} phases could be stable in all systems, but that there is a kinetic barrier to the L_α/Q_{II} transition in some systems, as has been suggested previously (Gruner et al., 1988; Shyamsunder et al., 1988; Anderson et al., 1988; Siegel and Banschbach, 1990). The possible nature of this kinetic barrier is treated later in this section (see the text beginning with the subsection, titled What determines whether ILAs and Q_{II} phases form spontaneously at $T < T_H$?). The fact that Q_{II} phases are not observed throughout the observed range of ILA stability (Gruner et al., 1988; Siegel and Banschbach, 1990) indicates that there are additional factors that determine the thermodynamic stability of these phases. These most likely include a chain-packing effect (Anderson et al., 1988), which is thought to be temperature dependent (Lewis et al., 1989; Siegel, 1993).

The effectiveness of temperature cycling in producing Q_{II} phases (Shyamsunder et al., 1988; Veiro et al., 1990; Tenchov et al., 1998) is easily understood in light of the stability of ILAs. If a system forms small numbers of ILAs each time it is heated through T_H, the ILAs will persist when it is cooled below T_H. After enough cycles, a sufficiently large fraction of the lipid will exist as ILAs to rearrange into a Q_{II} lattice (Siegel, 1986a; Siegel and Banschbach, 1990).

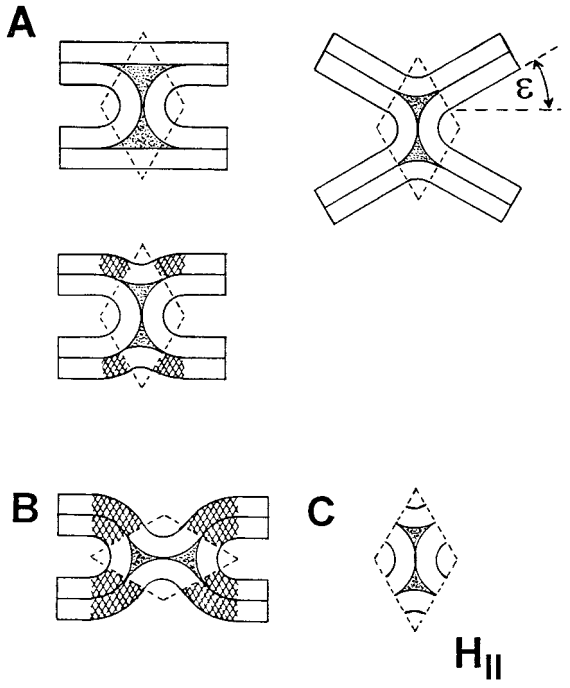

FIGURE 5 Comparison of the cross sections of (*A*) stalks and (*B*) a TMC, with the cross section of a unit cell of H_{II} phase (*C*). The cross section of a unit cell of the H_{II} phase is outlined in dashed lines in *A* and *B*. The regions of monolayer that are cross-hatched in *A* and *B* have unfavorable curvature energy. (Adapted from Siegel and Epand, 1997.)

How could L_α/H_{II} phase transitions proceed?

Now let us return to the question of how intermediates in the modified stalk theory might mediate the L_α/H_{II} phase transition. To transform into the H_{II} phase, all of the lipid monolayers in the lamellar phase have to be rolled up into tubes. As discussed previously (Siegel and Epand, 1997), the lowest energy, fastest pathway between the two phases would be to make a few small connections between apposed lipid/water interfaces in the lamellar phase and then lengthen them in the plane of the apposed bilayers into single units or domains of H_{II} phase, by diffusion of lipid from adjoining planar bilayers. Stalks and TMCs seem to be the lowest energy interbilayer structures that can form (Siegel, 1993), so we use these as models of the initial connections. Cross sections of stalks and a TMC are shown in Fig. 5, *A* and *B*, respectively. Note that the cross sections of the stalks and TMC all contain a region (*dashed diamond*) that is very similar to the cross section of an H_{II} phase unit cell (Fig. 5 *C*).

In L_α/H_{II} transition mechanisms like those proposed by Hui et al. (1983), Caffrey (1985), Siegel (1986a), and Siegel et al. (1994), stalks or TMCs could elongate in the plane parallel to the two apposed bilayer membranes to form a prism of H_{II}-like structure. These structures were referred to as "line defects" (Siegel, 1986a). The reasoning was that lipid in such a structure would have a chemical potential very nearly equal to that of lipid in the H_{II} phase, so at a temperature slightly above T_H, lipid would diffuse into the structure from the adjoining bilayer, lengthening it. These prisms would tend to align with other prisms forming between the same pair of bilayers (Siegel, 1986a) to assemble H_{II} phase domains.

The L_α/H_{II} phase transition does not occur via formation of line defects from individual stalks or TMCs

However, a transition mediated by line defects from isolated stalks or TMCs cannot rapidly form large domains of H_{II} phase. The analysis of Siegel (1986a) showed that line defects formed between the same pair of apposed bilayers could elongate rapidly and would tend to align with each other to form two-dimensional rafts of H_{II} tubes. However, there is no obvious mechanism by which the rafts formed between different pairs of bilayers could align with each other on a time scale of seconds or less to form three-dimensional arrays of H_{II} tubes. Thus it is hard to see how the transition could proceed via growth of line defects from individual stalks or TMCs.

More importantly, it was subsequently argued (Siegel and Epand, 1997) that individual stalks or TMCs cannot spontaneously grow into H_{II}-like line defects at temperatures near T_H and hence cannot be responsible for the rapid

transitions observed under those circumstances. A detailed analysis of this second point is given here.

Let us consider the two types of stalks that might evolve into line defects. In Fig. 5 *A*, the stalk at the top left has flat-topped interstices, and the stalk at the bottom left has dimpled interstices (see the Theoretical Methods). However, there are important differences between the cross sections of these structures and the cross section of the H_{II} phase unit cell (Fig. 5 *C*). A line defect structure with the cross section depicted at top left in Fig. 5 *A* has hydrophobic interstices that are nearly three times as large in cross section as in the H_{II} phase. The reduction in curvature free energy obtained by forming the curved interfaces in the H_{II} phase is more than offset by the energetically unfavorable creation of these larger interstices. Using the surface area scaling method to evaluate the energies of the interstices (Eq. A3), the free energy per unit length of such a line defect relative to the L_α phase, g_{LD}, would be

$$g_{LD} = 2\pi r\left(\frac{k_m}{2}\right)[(1/r - 1/R_0)^2 - 1/R_0^2] + 2[(\pi + 2)(r + h/2)]\gamma, \tag{4}$$

where the second bracketed term is the product of the perimeter of the interstice and the interstice "surface tension." At $T = T_H$, the value of r is very close to $/R_0/$ (Kozlov et al., 1994). Thus, using Eq. A3, Eq. 4 becomes

$$g_{LD} = -(\pi k_m/|R_0|) + 2(\pi + 2)(|R_0| + h/2)\gamma = 2k_m/|R_0|. \tag{5}$$

The free energy per lipid molecule in such a structure, relative to the free energy in the L_α phase, is g_{LD} divided by the number of lipid molecules entering this structure per unit length of extension, which is n_{LD},

$$n_{LD} = [2\pi|R_0| + 4(|R_0| + h/2)]/a. \tag{6}$$

Dividing Eq. 5 by Eq. 6 yields the free energy per lipid molecule in the interstice with flat-topped interstices with respect to the lamellar phase.

The free energy of a line defect growing from the stalk at the bottom left in Fig. 5 *A* can be calculated in similar fashion. In this case, the major difference in cross section between the stalk and the H_{II} phase unit cell is the positive-curvature regions of monolayer at the margins (*cross-hatched regions* in Fig. 5 *A*, *bottom left*). These positive-curvature regions are energetically unfavorable. The sum of the curvature elastic and interstice energy terms for a line defect of this second geometry is

$$g_{LD} = (\pi k_m/3)\left[\frac{1}{(r + h)} - \frac{2}{R_0}\right] + (\pi k_m/3)\left[\frac{1}{|r|} - \frac{2}{|R_0|}\right] + (\pi k_m/3)\left[\frac{1}{(|R_0 + h)|} - \frac{2}{|R_0|}\right] + 2g_{tsv}, \tag{7}$$

where g_{tsv} is the free energy of interstices bounded by monolayers of radius r (Siegel, 1993):

$$g_{tsv} = (\pi k_m/2r_H)(r/r_H). \tag{8}$$

The first, second, and third terms on the right side of Eq. 7 are the curvature energy of the curved *trans* monolayer margins of the cross section (*bottom left* of Fig. 5 *A*), the two dimples in the *trans* monolayer, and the two *cis* monolayer segments, respectively. Assuming $r = r_H = |R_0|$, as above, Eq. 7 becomes

$$g_{LD} = (\pi k_m/3)\left[\frac{1}{(|R_0 + h)|} + \frac{1}{|R_0|}\right], \tag{9}$$

and (by simple geometry) n_{LD} is

$$n_{LD} = (2\pi/3a)(5|R_0| + h). \tag{10}$$

Inspection of Eqs. 5 and 9 shows that g_{LD} for both hypothetical structures is positive with respect to the L_α phase, indicating that spontaneous growth of these structures will not occur at $T = T_H$. Using Eqs. 4–10, the free energies per lipid molecule in the line defects with cross sections at the top and bottom left of Fig. 5 *A* are ~0.14 and ~$0.12k_BT$ at $T = T_H$. Although these energies are small for every lipid molecule, the energies of the macroscopic lengths of such line defects (which would be needed to achieve the phase transition) would be very large indeed.

The only circumstances in which isolated stalks can elongate spontaneously into line defects at $T = T_H$ is when the local angle between the apposed interfaces (ϵ, *right-hand side* of Fig. 5 *A*) is 30°. However, this cannot be true at all places within the closely apposed bilayers of a bulk L_α phase: the bilayers would have to be deformed into 30° bends along the entire periphery of the growing line defect and be maintained in that configuration. This requires the input of additional energy and would prohibit the side-to-side aggregation of line defects that is necessary to form bulk H_{II} phase (Siegel, 1986a).

Although the cross section of a TMC (Fig. 5 *B*) also contains the cross section of a unit cell of H_{II} phase (*dashed lines*), the regions of bent bilayer at the periphery of the structure (*cross-hatched areas*) also have a large, unfavorable curvature energy. These regions are larger than the corresponding regions in stalk cross sections (Fig. 5 *A*, *left*), and it is easy to show that line defect growth from isolated TMCs takes even more energy than from isolated stalks. Therefore, elongation of TMCs also cannot be the mechanism of the L_α/H_{II} phase transition at T near T_H.

Experimental results support the analysis given here. In a previous temperature-jump time-resolved cryoelectron microscopy (TRC-TEM) study of bilayer/inverted phase transition mechanisms (Siegel et al., 1994), only very rare examples of line defects were observed. Interestingly, these rare examples occurred at the rims of contacts between apposed unilamellar liposomes, where the apposed bilayers met at angles of almost 30° (Figure 10 of Siegel et al., 1994). The present analysis shows that this is the only condition in which line defect formation is possible at $T \approx T_H$. Siegel et al. (1994) speculated that the absence of line defects at $T \approx T_H$ was due to a fast reversion of the line defects on the time scale of specimen cooling and vitrifica-

tion (~0.1 ms). In light of this subsequent analysis, isolated line defects are simply too unstable to form at $T \approx T_H$.

Formation of H_{II} phase precursors from aggregates of TMCs

Siegel and Epand (1997) previously suggested that TMCs could aggregate and form nuclei that could elongate into H_{II} phase domains. This proposal will be analyzed in more detail here.

The energy of isolated stalks and TMCs would be substantially decreased if the curvature energy of regions of monolayer at the periphery of the structures (*cross-hatched regions* in Fig. 5, *A* and *B*) could be reduced. For example, for a system like DOPE near T_H, two-thirds of the energy needed to form a TMC from L_α phase lipid goes into producing the curved bilayer regions at the periphery of the TMC. Side-to-side aggregation of two TMCs can reduce the free energy of these curved bilayer regions, lowering the free energy of the pair below the total of the energies of the isolated TMCs.

The aggregation process is depicted in Fig. 6. Fig. 6 *A* shows isolated TMCs forming within a stack of multilayers. A TMC (Fig. 6 *A*) is characterized by three parameters: the marginal radius r, the dimple radius r_3, and the marginal angle θ. The highest energy portion of the TMC is the "skirt" of bilayer corresponding to a range of θ of 60°–90°. It will be shown below that small reductions in the angle θ at any value of r substantially reduce the TMC energy, whereas small changes in r and r_3 have little effect on the energy of the TMC (Siegel, 1993). If two TMCs aggregate side by side as shown in Fig. 6 *B*, the area of "skirt" is reduced in the region of TMC contact. More importantly, the local value of θ at the TMC-TMC contacts is reduced from 90° to a figure close to 60° (*stippled area of bilayer* in Fig. 5 *B*). The local values of r and r_3 have to increase and decrease, respectively, to accommodate the local change in θ. However, the local spacing between bilayers around the periphery of the TMCs need not change to accommodate this local change in TMC geometry, since the sizes of r and r_3 can change in a complementary fashion around the circumference of the TMC. The aggregation process should continue in this pairwise fashion until an extended aggregate forms with a body-centered primitive tetragonal symmetry. Within this aggregate, each TMC has eight nearest neighbors: four arranged in a square around the "top" of the central TMC, and four around the "bottom." A cross section through this structure in the 110 plane is shown in Fig. 6 *C*. The shape of the array is complex, but it is similar to the geometry of the ILA array postulated as an intermediate in L_α/Q_{II} phase transitions (figure 3 *A* of Siegel, 1986c; figure 3 *C* of Siegel and Banschbach, 1990) and later observed via freeze fracture EM (Ellens et al., 1989; Siegel et al., 1989c). The major difference is that in the TMC array the catenoidal

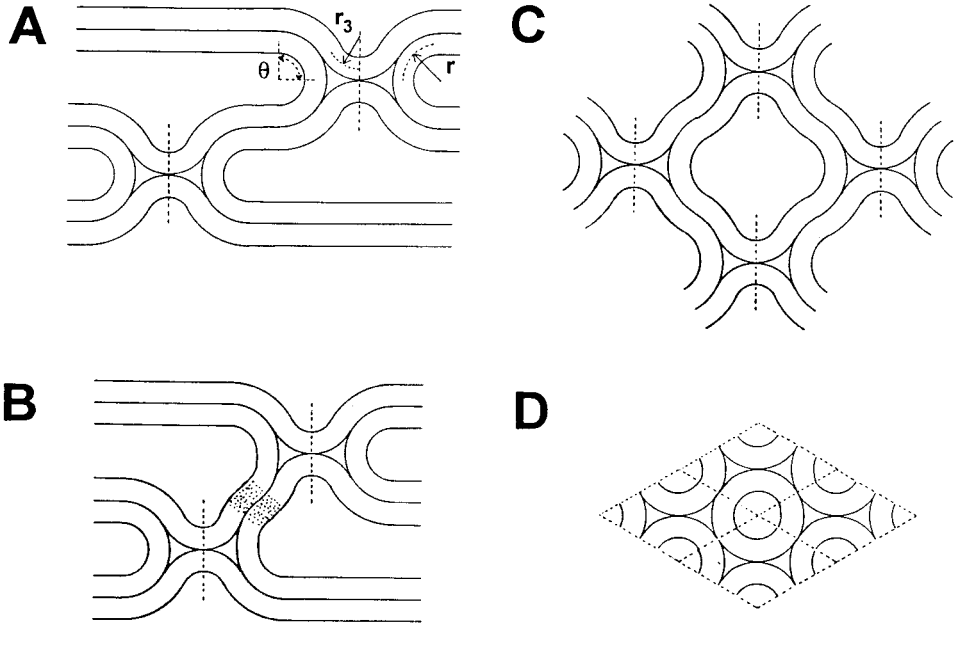

FIGURE 6 TMC aggregation into H_{II} phase precursors. (*A*) A pair of isolated TMCs in a stack of planar bilayers. The axis of each TMC is shown as a dashed vertical line. The marginal radius r, dimple radius r_3, and marginal angle θ are indicated. (*B*) Sideways aggregation of two TMCs reduces θ and increases r where they are in contact (*stippled area of bilayer*). The values of r and θ change in complementary fashion in the vicinity of the contact, so that the local spacing between bilayers around the periphery of the TMCs does not change. The process is driven by the large reduction in TMC energy achieved by locally reducing the value of θ (see text and Fig. 7). (*C*) The aggregation process proceeds to form a TMC aggregate with body-centered or primitive tetragonal symmetry. A cross section of this structure in the 110 plane is shown here. This cross section consists of closed cylinders of monolayer packed in quasihexagonal fashion (i.e., each cylinder has six nearest neighbors). At $T > T_H$, this structure could acquire lipid molecules by diffusion from adjoining bilayers and extend directly into a domain of H_{II} phase. (*D*) Cross section of a bundle of H_{II} phase tubes, to illustrate the similarity of the geometry in *C*. (Adapted from Siegel and Epand, 1997.)

interbilayer connections contain bilayer dimples instead of the water channels of the ILA array.

Energetics of TMC aggregation

The resulting shape of the TMC aggregate, or even of a pair of aggregated TMCs, is complex and hard to evaluate with our simple treatment (Siegel, 1993). However, it is shown here that two TMCs, in the process of diffusing toward each other, will spontaneously form the structure shown in Fig. 6 *B*. We compare the size of the gradients in free energy associated with changing each of θ, r, and r_3. This shows whether the reduction in free energy due to a local decrease in θ will be much more than enough to "pay" for the energy required to locally change r and r_3. The gradients are calculated for an isolated, undeformed TMC with $\theta = 90°$ at the minimum-energy dimensions in DOPE at $t = T_H$ (r = 3.7 nm, r_3 = 2.7 nm). The extent of the required changes in r and r_3 is estimated by assuming that the local spacing between bilayers does not change around the periphery of the aggregated TMCs. This is sensible, because it minimizes the amount of distortion necessary to make a stack of bilayers commensurate with the faces of a TMC array. Then it can be shown that the value of r at the sites of TMC-TMC contacts, r_c, is approximately

$$r_c \approx \frac{(r + h/2)}{\cos(\pi/2 - \theta)} - h/2, \tag{11}$$

and the value of r_3 at TMC-TMC contacts, r_{3c}, will be approximately

$$r_{3c} \approx r_3 - (r_c - r). \tag{12}$$

Fig. 7 shows plots of the energy of an isolated TMC subjected to changes in each of the three dimensions. Fig. 7 *A* shows that the energy of a TMC decreases rapidly and continuously with decreasing θ. The full line shows the curve for the equilibrium values of r and r_3. Reducing θ to ~60° reduces the energy by almost $45k_BT$. The size of this gradient is insensitive to the values of r and r_3. For example, Eqs. 11 and 12 were used to calculate the local values of r and r_3 necessary to achieve $\theta = 60°$ at the TMC-TMC contacts. Then the energy of an isolated TMC was evaluated as a function of θ with these values of r and r_3 around the entire periphery of a TMC. The results are the same to within $0.5k_BT$ at any θ. Fig. 7 *B* is a plot of the energy of an isolated TMC as a function of changes in r and r_3, respectively, given in terms of the values of r or r_3 needed to achieve a given value of θ between two aggregated TMCs. It is obvious that reductions in θ yield much greater reductions in TMC energy than the required changes in r and r_3: ~$45k_BT$ is obtained by reducing θ to 60°, but only ~5 or ~$6k_BT$ is needed to deform r and r_3 enough for that to happen. This shows that the aggregation process depicted in Fig. 6 *B* and *C*, will be spontaneous. Note that all of the curves in Fig. 7, *A* and *B*, are continuous and monotonic. This means that as two TMCs diffuse together, they continuously reduce their mutual energy as they form an aggregated pair: no activation energy is necessary for aggregation to occur. However, note that the TMC aggregate structure depicted in Fig. 6 *C* is energetically metastable. The energy of each TMC in such an aggregate is substantially lower than the energy of an isolated TMC but is still greater than an equivalent amount of lipid in the L_α phase.

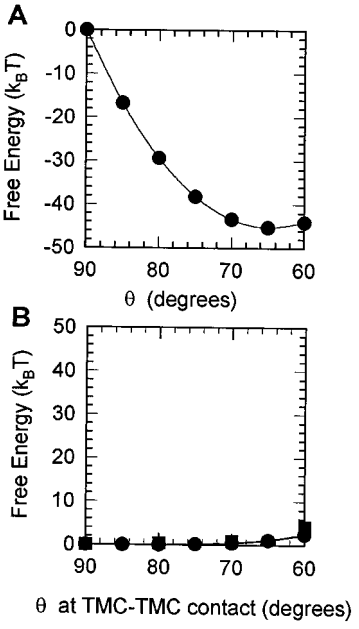

FIGURE 7 Energetics of TMC aggregation. (*A*) Plot of the change in energy of a TMC as the value of θ is decreased from 90° (i.e., from the value for an isolated TMC with $\epsilon = 0$). (*B*) For the local value of θ to be less than 90° between two aggregated TMCs, the local values of r and r_3 have to change. (*B*) Plot of the energy required to change r (*circles*) and r_3 (*squares*) for an entire TMC by the amount required to achieve the local value of θ indicated on the horizontal axis between two aggregated TMCs. Reductions in θ release much more energy than is required to achieve the required changes in r and r_3.

The driving force for aggregation of TMCs into clusters should also be affected by an entropic factor. To calculate the size of this factor, one needs accurate values for the difference in energy between aggregated and isolated TMCs. For the reasons given above, the present model gives only crude estimates of this energy. In addition, although stalks and TMCs seem to be the lowest energy intermembrane intermediates that can form, the energies of isolated TMCs calculated by this model are too large for a structure that must form in significant numbers to mediate the transition (see Discussion). This suggests that the energies for isolated TMCs may be inaccurate, and hence use of them to calculate TMC abundances and aggregation thresholds is inappropriate. The sole aim of the calculations here is to establish that there is a substantial driving force for TMC aggregation.

Consequences of spontaneous TMC aggregation

This array has two important properties. First, note that individual TMCs within the array cannot revert to planar

bilayer structure without also changing the structure of all of the surrounding TMCs: the value of θ for all of the neighbors must increase to 90°, and the data in Fig. 7 *A* show that this increases the energy of all of the neighboring TMCs. This means that the activation energy for reversion of each TMC in the array is larger (by $10–20k_BT$) than for reversion of isolated TMCs. Moreover, reversion of a TMC within the array involves coordinated motion in each of the neighboring TMCs, involving many more lipids in the reversion process than for reversion of an isolated TMC. Therefore, once an aggregate of TMCs forms, it should be kinetically metastable: it will endure for a much longer period of time than isolated TMCs. Even though the individual TMCs are unstable, the TMC array could endure for a macroscopic length of time.

The second important property of the TMC aggregate is its symmetry. Fig. 6 *C* shows that the cross section of the aggregate in the 110 plane has quasihexagonal symmetry. The cross section consists of closed, roughly cylindrical segments of monolayer packed in a hexagonal array (i.e., each cylinder has six nearest neighbors). This cross section resembles the cross section of a domain of H_{II} phase (Fig. 6 *D*). If the TMC aggregate is heated through T_H, lipid diffusion within the adjoining bilayers could cause this cross section to extend out of the plane of the paper, collapsing into a more perfectly hexagonal geometry as it extends, growing directly into a domain of H_{II} phase. The cross section in Fig. 6 *C* is essentially prisms of H_{II} phase unit cell connected by flat regions of L_α phase bilayers. Elongation of the structure at the expense of adjoining L_α phase bilayers should be spontaneous close to T_H. Therefore, Siegel and Epand (1997) proposed that this is the mechanism of the L_α-to-H_{II} phase transition: aggregates of TMCs constitute nuclei that grow directly into H_{II} phase domains by lipid diffusion.

The theoretical methods used to arrive at this mechanism (Siegel 1993) involve approximations. To simplify the mathematics, the intermediates are considered to have simplified geometries (i.e., to be made up of monolayer segments that are portions of spheres, cylinders, cones, or circular toroids of revolution). Related, but more complex, geometries like catenoids of ellipsoids of revolution may be involved, so that the predicted shape of the TMC aggregate is only approximate. The TMC aggregate may actually have a structure even more similar to the H_{II} phase than the structure depicted in Fig. 6 *C*.

Temperature dependence of TMC and TMC aggregate formation

Fig. 8 is a plot of the minimum TMC energy in the temperature interval below T_H. The energy changes by only 30% between $T_H - 20$ K and T_H. If TMCs are numerous at T_H, then substantial numbers of TMCs should form starting at temperatures well below T_H. Therefore, TMC aggregates should also be able to exist (at least transiently) at $T < T_H$. This is as observed (see below).

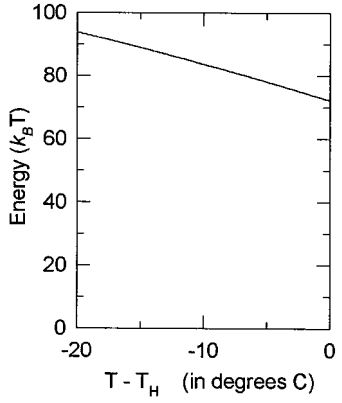

FIGURE 8 Energy of TMCs as a function of temperature below T_H.

TMCs and TMC aggregates should be more common in LUV than in MLV systems

As will be discussed below, there is some evidence for the TMC aggregation process depicted in Fig. 6. However, this evidence was obtained using a system in which the L_α/H_{II} transition was initiated in a suspension of large unilamellar vesicles (LUVs), as opposed to the multilamellar vesicle (MLV) systems in which the transition usually takes place (see below). Hence, before we consider this evidence, let us consider how the concentration or structure of the transition intermediates might be different in LUV versus MLV systems undergoing this phase transition.

TMC aggregates are expected (Siegel and Epand, 1997) to be larger and more numerous when the L_α/H_{II} phase transition begins with the lipid dispersed as LUVs. There are two reasons for this. First, the bilayers at the periphery of LUV-LUV contacts are curved, locally reducing ϵ for LUVs forming in these regions, which reduces the amount of energy necessary to form TMCs. Second, the value of the marginal radius, *r*, for TMCs (see Fig. 1 *C*) of minimum energy at $T = T_H$ is ~3.7 nm (Fig. 2 *A*). This results in an interbilayer spacing at the periphery of the stalk of between 5 and 6 nm. In contrast, the equilibrium water layer thickness between PE bilayers is only ~1 nm or less (Rand et al., 1988). The energy of a TMC that would "fit" between the lamellae within MLVs is more than twice as high as the energy of a TMC with larger values of *r*. MLVs are usually microns in extent. To form TMCs of minimal-energy dimensions, a lot of water would have to be transported through the many bilayers of the MLV, and within the planes between the bilayers. This would be a very slow process. In contrast, in aggregates of small (0.1 μ) LUVs, there are many water passages around the LUVs that reach the exterior of the aggregates, and the spacing between the apposed LUVs is initially much larger than in MLVs. For both of these reasons, TMCs should be more numerous and TMC aggregates larger and more plentiful when the L_α/H_{II} phase transition starts within aggregates of LUVs. Experimentally, it is not difficult to start the transition in dispersions of LUVs. PE LUVs can be made at high pH, where the

PE is charged, the LUVs do not aggregate, and the L_α/H_{II} transition cannot occur (Ellens et al., 1986, 1989). Acidification of the suspending buffer induces rapid aggregation of the LUVs, followed by intermediate formation and H_{II} phase formation if $T \geq T_H$ (Siegel et al., 1989c, 1994; Siegel and Epand, 1997).

There is experimental evidence that some types of long-range inverted phase order can be achieved more easily in LUV dispersions than in MLVs, as is proposed here for TMCs. The L_α/Q_{II} phase transition is more rapid in acidified LUV dispersions of DOPE-Me than in MLVs (Ellens et al., 1989). Freeze-fracture electron microscopy shows that acidified LUV dispersions form large domains of Q_{II} phase within 10 min or less after acidification, whereas MLVs incubated under similar conditions show only numerous ILAs and few if any Q_{II} inclusions. Moreover, light scattering and fluorescence data (Ellens et al., 1989) suggest that Q_{II} domain formation is more cooperative in LUVs than in MLVs and occurs within only 1–2 min. In contrast, Siegel and Banschbach (1990) showed that the L_α/Q_{II} phase transition in MLV samples takes ~1 h or more.

Experimental evidence for TMC aggregates and TMC aggregate-mediated L_α/H_{II} transitions in LUVs

Siegel and Epand (1997) studied the evolution of microstructure with time in acidified dispersions of DiPoPE LUVs via TRC-TEM. Their results show morphology that is consistent with the transition mechanism described in detail in the present work. Specifically, starting at temperatures as much as 38° below T_H, Siegel and Epand (1997) noted the appearance of many interbilayer structures of the same overall shape and size as predicted for TMCs (diameter ~10 nm). These structures tended to occur in large aggregates, which were usually disordered at lower temperatures. Unfortunately, the superposition of so many structures in the aggregates and the low contrast generated by such small structures in cryo-TEM (Siegel et al., 1994) did not permit demonstration of the detailed structure of the individual intermembrane structures, although they were clearly not ILAs. This is compatible with the prediction that TMC aggregates should exist well below T_H. With increasing temperature, the intermediates formed domains with quasihexagonal order that were tenths of a micron in diameter. In some projections, these domains resembled the cross sections of H_{II} phase domains, and arrays of bilayers with larger interbilayer spacings in others. These quasihexagonal domains formed at temperatures as much as 21° below T_H. These results suggest that the quasihexagonal domains correspond to the transition intermediate depicted in Fig. 6 *C*. Importantly, no evidence for isolated line defect-like structures was detected. As the temperature increased above T_H, the lipid aggregates showed a smooth transition to H_{II}-like order: the domains of intermediates increased in size and could not be distinguished from H_{II} phase. This is compatible with the suggested mechanism of H_{II} domain evolution from the quasihexagonal structure. Siegel and Epand (1997) also showed that the TMCs and TMC arrays were transient. ^{31}P NMR spectra were obtained from PE LUV dispersions within 1–2 min after acidification at temperatures several degrees below T_H. At these temperatures, quasihexagonal domains made up a large fraction of the specimens observed seconds after acidification by TRC-TEM. The NMR spectra showed only lamellar phase patterns, with occasional small isotropic components that decayed within minutes. Large numbers of TMCs or domains of quasihexagonal structure would have produced isotropic resonances. Therefore, the intermediate morphology observed via TRC-TEM decays within minutes or less. This is as expected, because the equilibrium phase under these circumstances is still the L_α phase.

However, the data in Siegel and Epand (1997) are subject to two caveats. First, the LUVs in Siegel and Epand (1997) had to be produced at high pH for technical reasons, where PE is unstable with respect to hydrolysis (S. Burgess, personal communication). Some, but not all, of the morphology observed by Siegel and Epand (1997) might correspond to H_{II} phases formed at lower temperature than in pure PE due to formation of some hydrolysis products (D. P. Siegel, work in progress). Second, there is some reason to believe that the effective T_H is lower for LUVs than for MLVs.

The free energy benefit of adsorption of one PE bilayer to another is substantial. When the bilayers can approach each other very closely, as in MLVs, the free energy of the MLV assembly is lower than that of well-separated isolated membranes, like those in LUV dispersions. The short-range interactions between PE bilayers (van der Waals forces and interbilayer hydrogen bonding) account for much of the adhesion energy (McIntosh and Simon, 1986, 1996; Rand et al., 1988). If the bilayers are maintained more than ~1 nm apart (as in LUV dispersions), the effective adhesion energy of the bilayers would be nearly zero (Rand et al., 1988), and the free energy per unit area of DiPoPE bilayers in LUV dispersions will be higher than for DiPoPE in MLVs. Formation of transition intermediates should require less activation energy and occur at slightly lower temperatures in LUV aggregates than in MLVs. Moreover, according to the present theory, H_{II} phases form from aggregates of TMCs, which keep the average interbilayer separation equal to 3 or 4 nm. Thus it is conceivable that for a small range of temperature below T_H, an H_{II} phase could be more stable than the bilayers in aggregates of LUVs but less stable than the bilayers in MLVs. This hypothetical H_{II} phase would form from the LUVs and then immediately decay back into L_α-phase MLVs. It is possible that some of the quasihexagonal morphology observed via TRC-TEM at $T < T_H$ actually corresponds to a metastable H_{II} phase. This possibility would also be compatible with the absence of nonlamellar ^{31}P NMR spectra 1 min after acidification of LUVs at $T < T_H$, because the metastable H_{II} phase formed under these circumstances would rapidly revert to more stable MLVs. Therefore it is important to calculate the extent to

which the free energy of bilayer-bilayer interaction could lower the transition temperature in LUVs.

Let the free energy of adhesion per unit area of one pair of PE interfaces be $-\Delta G_{ads}$. The free energy of adhesion per lipid molecule is then $-a\Delta G_{ads}/2$, where a is the area per lipid molecule at the bilayer/water interface. The free energy per lipid molecule in the bilayer of an LUV is then higher than that of equilibrium L_α phase (MLV) lipid by $a\Delta G_{ads}/2$. The free energy difference between H_{II} phase and L_α phase (MLV) lipid, ΔG_H, can be estimated by writing

$$\Delta G_H(T) \approx \Delta H_H - T\Delta S_H = \Delta H_H - T\left(\frac{\Delta H_H}{T_H}\right) = \Delta H_H\left(1 - \frac{T}{T_H}\right), \quad (13)$$

where ΔH_H and ΔS_H are the enthalpy and entropy of the transition per molecule, evaluated at $T = T_H$. The approximation used in the first equality in Eq. 13 is that the entropy change in forming the H_{II} phase at a temperature T is essentially the entropy change at $T = T_H$. This is a good approximation for a small temperature range around T_H, in which ΔH_H and ΔS_H can be considered to be roughly constant. The difference in free energy per molecule between LUV bilayer and H_{II} phase lipid is

$$\Delta G_{LUV} = \Delta G_H - \frac{a\Delta G_{ads}}{2}, \quad (14)$$

We can calculate the transition temperature for LUV lipid by setting $\Delta G_{LUV} = 0$ and using Eq. 13 to calculate the effective transition temperature for LUV lipid. It is easiest to express the result as the difference in transition temperature between LUV and MLV dispersions. Rearranging Eq. 14 and using Eq. 13, we find

$$\Delta T_H = (a\Delta G_{ads} T_H)/2\Delta H_H. \quad (15)$$

No measurements of ΔG_{ads} for DiPoPE are available. However, ΔG_{ads} has been measured for L_α phase POPE. For POPE, ΔG_{ads} is -0.15 erg/cm^2 (Evans and Needham, 1986, 1987). Calorimetric measurements of ΔH_H and T_H for DiPoPE yield values of 240 cal/mol (1.67×10^{-14} erg/molecule) and 43°C (316 K), respectively (Epand, 1985; Siegel and Epand, unpublished observations). With these values, and using $a = 0.65$ nm^2, we find that the value of ΔT_H is $-9°$ and that the "T_H" for LUVs would be ~34°C. Siegel and Epand (1997) observed quasihexagonal domains at temperatures as low as 21°C and clusters of intermediates (probably TMCs) at temperatures as low as 5°C. Therefore it is unlikely that this affect accounts for most of the quasihexagonal morphology observed in that work. However, this question will not be resolved until the value of ΔG_{ads} for DiPoPE is known.

TMCs and TMC aggregates may also mediate L_α/H_{II} transitions in MLV systems

Previous time-resolved x-ray diffraction (Caffrey, 1985; Kriechbaum et al., 1989; Caffrey et al., 1990; Laggner and Kriechbaum, 1991; Laggner et al., 1991; Erramilli et al., 1995; Tate et al., 1992; Erbes et al., 1997) and electron microscopy (e.g., Verkleij et al., 1978, 1979; Rand et al., 1981; Hui and Stewart, 1981; Hui et al., 1983; Verkleij, 1984) studies of the L_α/H_{II} phase transition revealed no evidence of ordered arrays of transient intermediates. This contrasts with the experimental evidence for such arrays when the phase transition occurs in LUV dispersions (Siegel and Epand, 1997). The x-ray and electron microscopy studies were done using MLV preparations obtained by direct hydration of dry lipid. TMCs and TMC aggregates should still form in such systems but would be less numerous, as discussed above. Rare TMC aggregates within MLVs could represent so small a fraction of the total lipid mass, or might be small enough (only a few lattice units in diameter), that they would not generate x-ray diffraction patterns strong or sharp enough to detect. The x-ray diffraction patterns would be determined by the bulk of the lipid in the sample. Similarly, freeze-fracture EM samples only a small fraction of the membrane in a dispersion (a single fracture plane). To determine if this is possible, we calculate the minimum number and size of TMC aggregates that could generate phase transition times compatible with observations on MLV systems.

To calculate the rate of a TMC-mediated phase transition, we first calculate the rate at which a given domain of TMC array can elongate into a domain of H_{II} phase. This is done by treating the individual tubes of the growing H_{II} phase domain. These tubes grow by the influx of lipid diffusing into the edges of the TMC array. The process corresponds to lipid flowing from regions of flat bilayer into regions with H_{II}-like curvature, with the curvature gradient occurring over a distance ~r, the marginal radius of the TMCs that make up the array. For small degrees of superheating, the free energy gradients accompanying this transport are small (~$0.001k_BT$ per lipid over several molecular widths for a superheating of 1 Kelvin above T_H), so that modeling this transport as a diffusive process is a crude but acceptable approximation. Using the same method as Siegel (1986a), we write the flux of lipid molecules across a border in a lipid monolayer of unit length as

$$J = (1/a)(D/k_BT)(\Delta G_H/\Delta x), \quad (16)$$

where D is the two-dimensional diffusion coefficient, ΔG_H is the change in chemical potential per molecule between lipid in the H_{II} and L_α phases, and Δx is the distance along the surface of the monolayer over which the lipid geometry changes from lamellar to H_{II}-like. We set $\Delta x = r$, note that each growing H_{II} tube can acquire lipid at both ends, and recall that the periphery of the monolayer in the H_{II} tube is

$2\pi r$. Then the total diffusive lipid flux into the H_{II} tube is

$$J_{tube} = (4\pi r/a)(D/k_BT)(\Delta H_H/r)\frac{(T - T_H)}{T_H}. \quad (17)$$

Simple geometry shows that the rate of elongation of an H_{II} tube is the total lipid flux into the tube divided by $(2\pi r/a)$. In Eq. 17 we have used Eq. 13 to express G_H in terms of the measurable quantities ΔH_H and T_H. We can then write an expression for the rate of elongation of an H_{II} tube at a temperature T:

$$dL/dt = (2D/k_BT)(\Delta H_H/r)\frac{(T_H - T)}{T_H} \quad (18)$$

For DOPE, ΔH_H and T_H are $\sim 0.492 k_BT$ and ~ 282 K, respectively (Epand, 1985). For $T = T_H + 1°$, $r = 3$ nm, and $D = 1 \times 10^{-7}$ cm^2/s, we find that $dL/dt \approx 12$ μm/s.

In most of the time-resolved x-ray diffraction studies of the L_α/H_{II} transition, the transition time has been on the order of 1 s for a heating rate of $\sim 1°$/s. We therefore calculate the number and size of the hypothetical TMC array domains that would be necessary to generate such a transition time. We assume that there are N_d TMC array domains per unit volume in the initial L_α phase, and that the domains are spheres of radius R_d. Then, using the value of dL/dt estimated above, we can write an expression for the approximate volume of L_α phase converted to H_{II} phase per second as

$$V_{trans} \approx \pi N_d R_d^2 (dL/dt). \quad (19)$$

If we require that the entire sample be transformed in 1 s ($V_{trans} = 1$ cm^3/s), then we find that $N_dR_d^2$ must be ~ 30 cm^{-1}. In LUV dispersions at temperatures 10° below T_H, the diameters of TMC array domains were often 0.2–0.3 μm in diameter (Siegel and Epand, 1997). Therefore, if we assume a smaller diameter of 0.1 μm for the MLV case, we find that N_d would have to be 1×10^{10}/cm^3. Multiplying N_d by the volume of each TMC domain, $(4\pi R_d^3/3 \approx 5 \times 10^{-13}$ cm^3 for spherical domains), we find that only $\sim 0.5\%$ of the total volume of the sample has to be present as TMC arrays for the phase transition to be complete within 1 s at $T = T_H + 1°$. Diffraction from such a small portion of the lipid might be too weak to be detected via time-resolved diffraction experiments on MLV systems. In addition, the TMC domains would be so small (10 lattice units in diameter) that the diffraction lines would be diffuse, compounding the problem of detecting them via x-ray diffraction.

What determines whether ILAs and Q_{II} phases form spontaneously at $T < T_H$?

According to the present model of the transition mechanism, TMCs either form ILAs (fusion pores, which assemble into Q_{II} phases) or, when the $T \geq T_H$, form aggregates that nucleate H_{II} tube formation. As one heats the L_α phase, the number of TMCs should increase as T approaches T_H, because the free energy of TMCs decreases as C_0 decreases with increasing T. At lower temperatures, isolated TMCs can either revert to planar bilayer structure or form ILAs, which leads to Q_{II} lattice formation. Aggregation of TMCs to form H_{II} phase precursors will be the dominant process at high temperatures, where the TMC concentration will be high. However, as discussed above, some lipid systems form ILAs and Q_{II} phases readily as they are heated, whereas in others, there seems to be a kinetic barrier to Q_{II} phase formation. In the latter systems, few ILAs and no Q_{II} phases are observed at conventional heating rates, or in the absence of temperature cycling, and the systems go directly from the L_α phase to the H_{II} phase. Why is this?

It might be argued that the relative ease of Q_{II} phase formation when the system is heated depends only on differences in the energy of TMCs near T_H in different lipid systems. Perhaps the TMC energy is higher in the systems observed to form Q_{II} phase, so that the steady-state TMC concentration is low below T_H. TMCs are less likely to aggregate at low temperatures, and more of them form ILAs and Q_{II} phase. However, in that case, there should also be a band of temperatures in which ILA formation is facile for the systems with lower TMC energies, farther below their corresponding T_H values. This is not what is observed: PEs do not form Q_{II} phases in the absence of temperature cycling (Tenchov et al., 1998) over large temperature ranges, including high absolute temperatures. Moreover, comparison of different lipid systems suggests that systems with very different Q_{II} phase-forming propensities should have similar TMC energies. The TMC energy is fixed by the values of k_m and C_0 of the lipid system. DOPE and DOPE-Me have very different Q_{II} phase-forming propensities (Gruner et al., 1988; Shyamsunder et al., 1988), but the values of C_0 for the two lipids, at their respective T_H, are very similar, and the rates of change of C_0 with T are also similar (Gruner et al., 1988). DEPE and DOPE-Me have roughly the same H_{II} phase lattice constant (7 versus 7.4 nm, respectively; Marsh, 1990) at T_H (64° versus 66°C, respectively; Marsh, 1990), indicating that these two lipids have nearly the same C_0. However, DOPE-Me forms Q_{II} phases spontaneously at slow heating rates (Siegel and Banschbach, 1990), whereas DEPE does not form Q_{II} phases unless temperature cycling is applied (Tenchov et al., 1998). Finally, mixtures of DOPE with low mole fractions of DOPC form ILAs in large numbers (Ellens et al., 1989), whereas DOPE does not. The k_m of DOPC is almost 20% smaller than that of DOPE (Chen and Rand, 1997), which would make k_m lower in the DOPE/DOPC mixture relative to DOPE, not higher. The C_0 of a DOPE/DOPC = 3/1 mixture is within 8% of that of pure DOPE (Tate and Gruner, 1989) at the temperature where numerous ILAs are observed (Ellens et al., 1989). Therefore, although differences in TMC energy between different systems may play a role, there is probably another factor accounting for the kinetic barrier to Q_{II} phase formation.

Alternatively, there may be differences between lipid systems in the inherent rate of ILA formation from isolated

TMCs. If isolated TMCs immediately decay into ILAs at any TMC concentration, Q_{II} phase formation should be facile, and the sequence of phases with increasing T will be L_α, Q_{II}, and H_{II}. If isolated TMCs rarely form ILAs, then few ILAs will form while $T < T_H$, and the Q_{II} phase will form very slowly, perhaps too slowly to be observed at most experimentally convenient heating rates (e.g., DOPE-Me; Siegel and Banschbach, 1990). This seems a more likely explanation. It is also consistent with the effects of low levels of peptides on Q_{II} phase formation (see Discussion).

Kinetic and energetic barriers to ILA formation

If the kinetic barrier to Q_{II} phase formation in some systems is due to a slow rate of conversion of TMCs to ILAs, then the rate of TMC decay to ILA structure must be affected by factors other than the geometric mean curvature elastic and interstice energies. Two such factors come to mind. The first is the rupture tension of the bilayer diaphragm of the TMC. The rupture tension is the energy per unit area required to rupture a bilayer of the given lipid composition (Evans and Needham, 1986, 1987). The second factor is the Gaussian curvature elastic modulus of the lipid composition. This factor affects the relative energy of the ILA with respect to planar bilayer, the TMC, and the H_{II} phase (Siegel, 1993). Positive Gaussian curvature elastic moduli favor formation of ILAs from TMCs by increasing the driving force for this process. At present there is controversy over the magnitude and sign of the Gaussian curvature elastic modulus in polar lipid systems (Chung and Caffrey, 1994a, b; Templer et al., 1994) and even some question about whether the modulus can be measured accurately with present methodologies (Templer, 1995). In the absence of more quantitative data, we concentrate on the effects of membrane rupture tension.

The possible role of bilayer rupture tension in ILA formation and membrane fusion

For a TMC to form an ILA, the bilayer dimple in the center of the TMC must rupture, forming a transient pore that widens to form the inner walls of the ILA channel (Fig. 1 *C* and *left side* of Fig. 1 *D*). This bilayer dimple is under considerable curvature and interstice energy stress (Siegel, 1993). The susceptibility of planar bilayers to rupture and pore formation is determined by the bilayer rupture tension, τ, which is the membrane tension that has to be applied to a bilayer of the given lipid composition to rupture it (Evans and Needham, 1987). Because the initial steps in planar bilayer rupture should resemble pore formation in the diaphragm of the TMC, Siegel and Epand (1997) postulated that the magnitude of τ could also determine the susceptibility of the TMC diaphragm to rupture under stress. The same assumption is made here. It has to be noted that the planar bilayer is under a form of stress (dilatational) different from that on the TMC diaphragm, which is under curvature and interstice energy stress. However, because the initial pore formation in the rupture event in the two cases is presumably similar, the magnitude of τ gives at least a measure of the inherent susceptibility of a TMC diaphragm of the same lipid composition to rupture.

τ is a material property determined by the details of the interaction between adjacent molecules in the bilayer. It is therefore sensitive to changes in molecular structure in a way that is different from that of the curvature elasticity modulus, k_m. In lipid compositions with large values of τ, TMCs would be more resistant to dimple rupture and ILA formation, and hence would be less likely to form Q_{II} phases, than compositions with small values of τ. τ can be measured by mechanical manipulation of liposomes, and it is found to be sensitive to bilayer composition (reviewed in Evans and Needham, 1987). For instance, the inclusion of 1 mol% of a hydrophobic peptide decreases τ of SOPC bilayers to roughly one-half the value for pure SOPC (Evans and Needham, 1987), and the inclusion of 50 mol% monooleoyl-PC in egg PC bilayers reduces τ by a factor of 500 (McIntosh et al., 1995). τ is correlated with the area compressibility modulus of the bilayers. It is therefore interesting that, as one increases the mole fraction of PE in PC bilayers, this modulus increases (Evans and Needham, 1987). This implies that pure PE has a higher value of τ than PE-PC mixtures, which would be consistent with the observed tendency of PE-PC mixtures to form Q_{II} phases, compared to pure PE (e.g., Ellens et al., 1989).

Changes in TMC diaphragm stress as a function of temperature

As the temperature increases, the stress on the diaphragm of a TMC decreases. This might reduce the tendency of TMCs to form ILAs at high temperature, favoring H_{II} phase formation at $T \approx T_H$. Using equations derived in Siegel (1993), it can be shown that the values of r_3 and r for a minimum energy TMC increase as C_0 decreases. This has the effect of reducing the stress per unit area of monolayer in the TMC diaphragm. The temperature dependence of the diaphragm stress is plotted in Fig. 9. For comparison, pure phospholipids have bilayer rupture tensions of ~3–7 mN/m (Evans and Needham, 1986, 1987; Longo et al., 1997). The values calculated here are probably overestimates, because there is a large curvature gradient across the *trans* monolayers of the TMC, and in reality the stress per unit area is partially relaxed by changes in local lipid density and slight changes in TMC shape. Moreover, as T gets close to T_H, TMCs also show a slight tendency to expand radially, producing a diaphragm of planar bilayer in the center of the dimple with a radius R_x and a slight tendency to grow in the r dimension. These changes are depicted in Fig. 10. Radial expansion by a few tenths of a nanometer lowers the TMC energy a further few percent at $T \approx T_H$, if r is nearly constant. The reduction in energy is larger if both r and R_x are permitted to increase, the extent depending on the value of ϵ. At T_H,

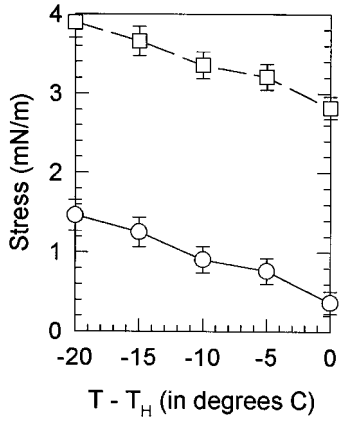

FIGURE 9 Stress per unit area on a TMC diaphragm as a function of temperature below T_H. Squares: Stress per unit area, including the effects of interstice energies. Circles: Stress per unit area, including only the effects of curvature energy. The stress per unit area is very sensitive to r_3: the error bars indicate the changes made by a 0.05-nm change in r_3 (the increment used in calculating these results).

a TMC can lower its energy by $\sim 10-18 k_B T$ if R_x and r increase by 1–2 nm. The gradient in TMC energy as a function of increasing r and R_x is very shallow beyond this point. Further expansion of r is probably inhibited by the restrictions imposed by the L_α host lattice. The expansion slightly distorts the TMC array geometry, as depicted in Fig. 6 *C*: the cross section of the unit cell becomes a rhomboid with slightly different dimensions but the same overall geometry. This effect does not interfere with the transition mechanism depicted in Fig. 6, as the unit cell cross section of the expanded TMC array is still qualitatively and quantitatively similar to the cross section of a nascent H_{II} phase domain.

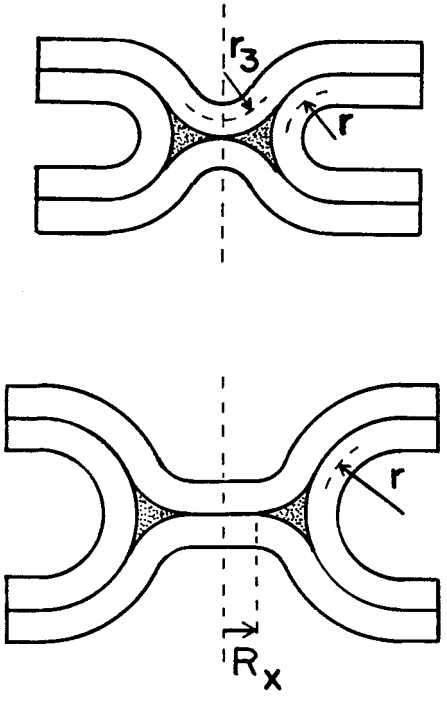

FIGURE 10 Expansion of TMCs near T_H. The energy of isolated TMCs can be reduced slightly by formation of a small area of planar bilayer diaphragm in the center of the diaphragm, with a radius R_x, accompanied by an increase in the marginal radius, r.

Mechanisms of the H_{II}/L_α and Q_{II}/H_{II} phase transitions

The proposed L_α/H_{II} and L_α/Q_{II} phase transition mechanisms also provide some insight into the mechanisms of other transitions within this set of phases. The mechanism of the H_{II}/L_α transition presumably resembles contraction of H_{II} domains into TMC aggregates. However, the rate of this transition will be strongly influenced by the density of defects in the H_{II} phase. If the domains of H_{II} phase have "ends" that retain structure resembling a bit of the TMC array in Fig. 6 *C*, the reverse transition should be facile. If these defects have to be produced by localized fission of several H_{II} tubes, then the transition could be slower than the forward transition for similar extents of supercooling and superheating. The Q_{II}/H_{II} phase transition may occur via a mechanism related to TMC array elongation into H_{II} phase. The ordered array of TMCs postulated by the present L_α/H_{II} transition mechanism has the same symmetry as the ILA array postulated (Siegel, 1986c) and observed (e.g., Ellens et al., 1989; Siegel et al., 1989) as an intermediate in the L_α/Q_{II} transition mechanism and is similar in overall symmetry to the Im3m Q_{II} structure (Siegel, 1986c). The Q_{II}/H_{II} transition occurs at temperatures well above T_H (e.g., as for DOPE-Me), and the size of the Q_{II} phase unit cell decreases with increasing temperature. It is possible that as the diameter of the water channels of the Q_{II} phase shrink with increasing temperature, the interfaces of the channels may be able to fuse locally and form TMC-like connections between the linings. A cross section through a Q_{II} phase domain with many such TMC-like channel closings may correspond to a hexagonally packed monolayer cylinder geometry like the one depicted in Fig. 6 *C* and therefore may elongate directly into an H_{II} phase domain.

DISCUSSION

A stalk-based mechanism is compatible with most observations concerning lamellar/inverted phase transitions in uncharged lipid systems. In this model, stalks are the first intermembrane structures to form. Stalks then evolve into TMCs, which rupture to produce ILAs (fusion pores) or aggregate to produce H_{II} phase domains. TRC-TEM evidence shows what appear to be the TMC arrays predicted by the theory at temperatures around T_H in DiPoPE (Siegel and Epand, 1997). This provides substantial evidence for the existence of TMCs. Therefore, these experimental and theoretical results both support the modified stalk theory of membrane fusion in uncharged lipid systems (Siegel, 1993)

and strongly suggest that the same mechanism is involved in lamellar/inverted phase transitions.

Compared to earlier proposals (Hui et al., 1983; Caffrey, 1985; Siegel, 1986a), the new element in the model of H_{II} phase formation is that H_{II} domains are created by lateral extension of arrays of TMCs. H_{II} domains with long-range order (bundles of H_{II} tubes 0.1–1 μm in diameter) grow directly from these TMC arrays. This is compatible with extremely rapid formation of H_{II} phase domains observed under some conditions (i.e., domains formed within 10 ms or less in highly superheated samples; Siegel et al., 1994). TRC-TEM data (Siegel and Epand, 1997) indicate that the putative TMC arrays are metastable at $T \approx T_H$, enduring for seconds, at least when they form from aggregating unilamellar liposomes. It is possible that these arrays would be detectable via other time-resolved techniques such as synchrotron source x-ray diffraction. However, as noted in the Results (subsection titled Experimental evidence for TMC aggregates and TMC aggregate-mediated L_α/H_{II} transitions in LUVs), there are some caveats regarding the intermediate morphology observed by Siegel and Epand (1997).

The new model of Q_{II} phase formation is different from an earlier proposal (Siegel, 1986c) in two ways. First, ILAs are postulated to arise from TMCs rather than inverted micellar structures. Second, it is shown that ILAs are lower in energy than the L_α and H_{II} phases in a broad interval of temperatures around T_H. This means that ILAs and the Q_{II} phases that form from them (Siegel, 1986c; Siegel et al., 1989c) should be thermodynamically stable in this interval for all systems with thermotropic transitions. The earlier model (Siegel, 1986c) could not yield quantitative estimates of the relative energies of ILA planar bilayers.

The model predicts that ILAs can start to form at very low temperatures (T_c) and persist up to ~13 K above T_H for lipids with the properties of DOPE. As mentioned in the Discussion, ILAs are observed starting ~30–40 K below T_H and to at least 14 K above T_H in DOPE-Me, which is a very similar lipid system. This is surprisingly good agreement, considering the simplicity of the treatment. The onset temperature for ILA formation predicted here is an underestimate for several reasons. TMCs may not form in sufficient numbers at such low temperatures (near 0°C for DOPE-Me) to permit a detectable level of ILA formation. Moreover, R_0 probably increases more rapidly with decreasing temperature than indicated by Eq. 1, and k_m probably increases as well. This would raise the energy of ILAs at lower temperatures relative to the current model and thus raise the onset temperature for ILA formation. However, it should also be noted that the techniques used to detect ILAs are incapable of detecting them in small numbers, so a few ILAs may form at temperatures below the reported onset temperatures.

The model of ILAs in this work is simplistic. To make the mathematics tractable and eliminate parameters, ILAs are assumed to be circular toroids of revolution. Structures of this geometry would have curvature gradients on their surfaces, and they would probably deform so as to reduce those gradients. In particular, if there are many ILAs in a stack of bilayers, the ILAs may adopt a geometry based on a recently discovered infinite periodic constant-curvature surface. The units of this structure have the same general shape as ILAs (figure 3 in Thomas et al., 1988), but the monolayers would have lower, more uniform curvature. Bilayer structures based on such constant-curvature surfaces are also subject to a chain-packing constraint (Anderson et al., 1988), absent from the simplified model used here. The constraint arises from the need for the two monolayers of the constituent bilayers to lie on surfaces of constant curvature. The local thickness of the monolayers must vary across the unit cell to meet this constraint, which destabilizes the structure relative to the L_α phase. The size of this effect is estimated to be a small fraction of the interstice energy of the H_{II} phase (Anderson et al., 1988). Finally, ILAs have a lower Gaussian curvature elastic energy than flat bilayers or the H_{II} phase (Siegel, 1993). However, at present reliable values of the Gaussian curvature modulus for pure phospholipids are not available. In the Appendix the order-of-magnitude effects of chain-packing and Gaussian curvature elastic energies of the temperature range of ILA array stability are calculated. The two effects can each change the upper temperature limit by only several degrees, but can easily change the lower temperature limit by tens of degrees. In sum, the model of the ILA used in this work is crude. Accordingly, the temperature interval calculation here is intended only as a rough check on the theory.

The model predicts that all thermotropic systems should form ILAs and Q_{II} phases at equilibrium. This implies that there is a kinetic barrier to Q_{II} phase production in some systems (see Results, section titled Comparison of predictions and observations concerning Q_{II} phase stability). The nature of this kinetic barrier is not indicated by the model, which deals only with the curvature elastic and interstice packing energies of the intermediates. Because ILAs are observed to be stable once formed (see Results), it is suggested that the kinetic barrier occurs in part at the step of TMC rupture to form ILAs. Composition-dependent changes in the lipid bilayer rupture tension or the Gaussian curvature modulus could be responsible for the occurrence of rapid L_α/Q_{II} transitions in some systems and not in others. Changes in the Gaussian curvature modulus affect the relative stability of ILAs and TMCs (Siegel, 1993) and hence change the driving force for TMC rupture.

The bilayer rupture tension, τ, may determine the relative rate of ILA production and hence the rate of ILA and Q_{II} phase production. Systems with large values of τ should form ILAs slowly and have facile L_α/H_{II} transitions, whereas systems with small values should form more ILAs and thus form Q_{II} phases. The small amount of τ data available are consistent with the observed behavior of PE, PE/PC, and *N*-monomethylated PE systems (Evans and Needham, 1986, 1987). It is possible that τ is an important variable in membrane fusion in general, if a stalk/TMC mechanism is involved. This should be tested in pure lipid systems, comparing the effects of low mole fractions of agents that change τ while making minimal changes in C_0.

As noted previously by Siegel and Epand (1997), very low mole fractions of some hydrophobic or amphipathic peptides drastically change τ (Evans and Needham, 1986, 1987; Longo et al., 1997), and very low mole fractions of some amphipathic peptides induce Q_{II} phase formation (Keller et al., 1993, 1996; Colotto et al., 1996; Morein et al., 1997) without having significant effects on C_0 (Colotto and Epand, 1997; also as discussed in Siegel and Epand, 1997). This suggests that peptides could be used to study the effects of τ on the rates of Q_{II} phase formation and membrane fusion. Interestingly, some of these peptides are so-called fusion peptides from viral proteins that induce membrane fusion (Colotto et al., 1996; Colotto and Epand, 1997; Longo et al., 1997).

There is also an interesting suggestion by Fournier (1996) that asymmetrical objects, including amphipathic peptides, that bind to both sides of a bilayer could induce negative Gaussian curvature. In this way, amphipathic peptides may induce Q_{II} phase formation by increasing the driving force for ILA formation, instead of or in addition to a kinetic effect like a reduction in rupture tension of the bilayer. However, near T_H the energy gradient between TMCs and ILAs is already huge (Figs. 2 and 3). Thus, to this author, an effect of peptides on τ seems to be the more likely of these two possibilities. Extensive studies of the effects of peptides on lipid phase behavior, phase structure, and lipid membrane rupture are required to resolve this question.

The current theory is only applicable to systems in which electrostatic contributions can be neglected (low mole fraction of charged lipids and ionic strengths of 0.1 M or more). Otherwise, electrostatic contributions to the intermediate energies could be substantial, and the mechanism of fusion may even be different from the one elaborated on here. Some biomembranes contain substantial mole fractions of charged lipids. It is therefore important to develop an understanding of charged lipid effects on fusion intermediate structure and to develop better experimental methods for studying intermediate structure.

Finally, the energies of the TMC intermediate in this work are high ($\sim 72 k_B T$ for DOPE at $T = T_H$) for a structure that must form in substantial numbers, if it is to mediate lamellar/inverted phase transitions. This creates a dilemma. Stalks and TMCs are the lowest-energy intermembrane structures that have yet been proposed (Siegel, 1993). Transient morphology consistent with the stalk/TMC hypothesis has been observed (Siegel and Epand, 1997), although the data do not directly demonstrate the fine structure of the intermediates. It is currently difficult to see how any intermembrane structure could have a lower energy, assuming that our model for the energies of monolayer-based assemblies is correct. Stalks and TMCs combine the qualities of minimum size and compound curvature, the two critical components for structures with minimal curvature elastic energy (Siegel, 1993). The model used here for the energy of monolayer structures is surprisingly accurate in quantitatively reproducing the DOPE-water phase diagram (Kozlov et al., 1994). The present analysis also provides a fairly good prediction of the temperature range for ILA existence. Both of these facts imply that our model of intermediate energies is not missing large factors. Inclusion of Gaussian curvature elastic energy in the present model would probably not change stalk and TMC energies by more than $\sim 5 k_B T$ (see Appendix). Thus it is troubling that the energies predicted for stalk and TMC intermediates are so high.

The basis of this apparent dilemma may reside in three aspects of the present model. First is the model's use of quadratic curvature elastic expressions (equation 1 of Siegel, 1993) for structures like stalks and TMCs, which have compound ("saddle") curvature and small principal radii of curvature. The quadratic curvature elastic model used here appears to be accurate in predicting the relative free energies of the H_{II} and L_α phases (Kozlov et al., 1994), which lack compound curvature. It may be that in monolayers with compound curvature and principal radii of curvature that are close to molecular lengths (as in stalks and TMCs), higher-order curvature terms are needed to express the curvature elastic energy. Second, the present method for estimating the interstice energies of TMCs may be deficient. At $T = T_H$, the total curvature energy of the TMC is nearly zero, and the calculated energy is essentially the interstice energy. The radius of the interstice in the plane of the TMC circumference is small, and multiplying the circumference of the TMC centroid by the energy of the linear interstice in H_{II} phases may overestimate the interstice energy. Calculating the interstice energy using the "interfacial tension" model (see Appendix I) does not reduce this energy, but this may be due to an overestimation of the surface area of the interstice in the idealized geometry of the present model. (Because of the assumed circular toroid geometry, much of the "surface area" of the interstice lies at the rims of the interstice, where the two lipid/vacuum "interfaces" would be less than 0.1 nm apart, a situation in which the two interfaces cannot be defined.) Third, a number of assumptions had to be made to make the mathematics tractable and to prevent parameterization. The current treatment assumes that lipid monolayers maintain a constant thickness across highly curved surfaces, that the midplane of the monolayers is at a constant depth within the monolayer, and that there is no area elastic contribution to the energy. All of these assumptions are to some degree unrealistic. For instance, there may be coupling between monolayer thicknesses or chain tilting and curvature that are not accounted for here. In addition, the geometric model used for some surfaces of stalks and TMCs (circular toroids) may be a gross simplification. The energies of these structures are sensitive to the local value of ϵ (Fig. A1), and the surfaces of this geometry would have large curvature gradients. These two facts imply that the corresponding surfaces in real intermediates would deform into different shapes with lower free energies (e.g., like the surface in figure 3 of Thomas et al., 1988). Experimental work on the relative stability of Q_{II} and L_α phases and improved theoretical models of monolayer deformation are necessary to resolve these questions.

However, note that even if the expressions for the absolute energies of high-curvature, compound curvature surfaces are poor estimates, or if the estimates of the interstice energies of TMCs are inaccurate, this would not invalidate

the chief results of this work. These are the predicted thermodynamic stability of ILAs and Q_{II} phases; the common pathway to H_{II} and Q_{II} phase formation via TMCs; and the driving force for nucleation of H_{II} phase domains from aggregates of TMCs. The driving force for TMC aggregation is the reduction in curvature energy of the bent bilayer margins of aggregated versus isolated TMCs. As shown in Fig. 7 *A*, this reduction is substantial even for small values of ϵ, corresponding to bilayer regions with modest curvature, where the quadratic curvature energy expression is likely to be quantitative.

TMCs forming between biomembranes would probably have lower energies than the values computed via the present model. Biomembranes contain low mole fractions of apolar lipids like triglycerides and dolichol. These oils would reduce the interstice energy of TMCs, just as apolar oils reduce the interstice energy of H_{II} phases (Kirk and Gruner, 1985; Tate and Gruner, 1987; Sjölund et al., 1987; Siegel et al., 1989b). This would lower the energy of TMCs by up to $50-80k_BT$ below the values calculated for any given value of C_0. In the presence of apolar oils, radial expansion of TMCs (Fig. 10) could also proceed more easily. However, the stress per unit area on the TMC diaphragm is at maximum before radial expansion, so that even in such cases, rupture to form fusion pores probably occurs before extensive expansion occurs.

APPENDIX 1: THEORETICAL METHODS

Outline

Calculations were performed using the same methods and equations given by Siegel (1993). (One equation in Siegel (1993) contains a typographical error. In equation A1 of that work, arguments of the inverse tangent function should be $X \tan(\theta/2)$ instead of $X \tan(\theta)$. However, the calculations in Siegel (1993) were performed with the correct form of the equation.) In outline, the method assumes that the energy of a monolayer-based structure with respect to the L_α phase at the same temperature is a sum of a curvature elastic energy and an interstice energy. Both of these components can be evaluated using x-ray diffraction data from a reference system with the same acyl chain composition at the same temperature. There are no adjustable parameters in the theory. The principle assumptions are 1) that the contributions of electrostatic and hydration energies can be neglected as a function of monolayer curvature; 2) that the energies of different monolayer segments can be evaluated separately and summed; 3) that the thickness of the lipid monolayers is independent of their curvature; 4) that the geometries of monolayer segments are well approximated by segments of spheres and circular toroids; 5) that the geometric mean curvature elastic modulus is constant across the relevant temperature range; and 6) that the interstice energy is independent of the spontaneous curvature, C_0, for a homologous series of lipids if the acyl chains are the same and all of the lipids have a similar chain-melting temperature T_c, for $T > T_c$. The last is fulfilled by a series of mixtures of DOPC and DOPE or DOPE-Me, for example.

The general method has been validated by the recent work of Kozlov et al. (1994). They showed that a method using the same principal elements successfully reproduces a complex part of the phase diagram of DOPE/water over a substantial range of water concentration and temperature. As in much previous work (e.g., Markin et al., 1984; Chernomordik et al., 1985; Leikin et al., 1987; Kozlov et al., 1989; Nanavati et al., 1992; Siegel, 1993), the curvature energy calculations in this work only take into account terms that are quadratic in curvature. In addition, curvature is evaluated at the monolayer midplane, because that is the approximate location of the neutral surface in phospholipid systems (e.g., Leikin et al., 1996). However, it should be noted that higher order curvature terms and coupling of bending elasticity to area deformation may be important in some geometries, and that the neutral surface may move as a function of the extent of deformation (e.g., Kozlov and Winterhalter, 1991a,b; Leikin et al., 1996). To keep the mathematics tractable and avoid the introduction of coupling parameters, we assume that the simple procedure is applicable to one-component lipid systems at full hydration.

The effects of Gaussian curvature elasticity are neglected. However, if the relevant curvature constant is known, the contributions of Gaussian curvature energy are easy to calculate (Siegel, 1993). If we include the Gaussian curvature contribution, the energies of stalks and TMCs would be lower than values calculated here by an amount equal to $4\pi\kappa_G$ (Siegel, 1993), and ILAs by $8\pi\kappa_G$, where κ_G is the Gaussian curvature elastic modulus. Note that the sign of κ_G could be either positive or negative.

The relative energies of intermediate structures are calculated using parameters measured for DOPE. The major difference in the calculations here and in Siegel (1993) is that the values of the curvature elastic constant, k_m, and the radius of the lipid monolayer in the H_{II} phase at T_H, r_H, are the revised experimental values for this system obtained by Kozlov et al. (Kozlov and Winterhalter, 1991b; Kozlov et al., 1994) from the original data collected by Rand et al. (1990). The revised values of k_m and r_H (Kozlov et al., 1994) are 4.2×10^{-13} erg and 2.87 nm at 295 K, respectively. The revised value of k_m is ~50% of the value used in Siegel (1993), which was based on an earlier analysis (Rand et al., 1990). Because the energies of all of the intermediates calculated in Siegel (1993) are all directly proportional to k_m, the energies should be reduced by this factor. Here the revised value of r_H is used as the radius of the monolayer midplane because this greatly simplifies the calculations. In fact, the position of the neutral plane and the midplane may differ by as much as 0.3 nm (Kozlov and Winterhalter, 1991b; Rand et al., 1990). The energies are calculated as the difference between the energy of the intermediate structure and an equivalent area of monolayer in the L_α phase at the reference temperature, 295 K. The energies are in units of k_BT, where k_B is Boltzmann's constant and T is 295 K, the temperature at which k_m and r_H were measured (Rand et al., 1990). No measurements were made at T_H (283 K; Epand, 1985; Gruner et al., 1988), so these values of k_m and r_H are taken to be the values at T_H.

The effects of lipid composition and temperature on intermediate energies are modeled by changing the value of C_0. The temperature dependence of C_0 for DOPE has been obtained from x-ray diffraction studies of DOPE H_{II} phases at full hydration (Tate and Gruner, 1989; Tate et al., 1992). Changes in lipid composition can be accommodated by using a mole fraction weighted sum of the C_0 values for each of the pure components (Keller et al., 1993). Here we will be concerned chiefly with one-component lipid systems.

In calculating the energies of fusion intermediates, some authors (e.g., Chernomordik et al., 1995a, b; Chernomordik and Zimmerberg, 1995) neglect the curvature energy of the distal, nonapposed monolayers of the intermediates. The calculations in Siegel (1993) show that the curvature energy of the distal monolayers is a substantial contribution to the total energy and is sometimes the dominant contribution. If it is neglected, the total energy of the intermediate is underestimated. As in previous work (Siegel, 1993), the curvature energy of the distal monolayers of stalks and TMCs is included in the results reported here. The curvature energy of the *cis* monolayers of the stalk structure is greatly reduced by radial expansion, and the distal monolayers must deform inward to prevent formation of a vacuum during this expansion. If the distal monolayers remained planar during radial expansion of the *cis* monolayers and a vacuum is left inside the structure, the interior surfaces of the distal monolayers would line this cavity. These interfaces would resemble the interface between long-chain alkanes and vapor. The surface tension of long-chain alkanes ranges from 20 to 27 erg/cm^2 (Small, 1996). This would make the energy of such a structure many times larger than the energy of a TMC of corresponding size, and in fact an "interfacial tension" of only 1 erg/cm^2 at these interfaces is sufficient to enforce inward dimpling of the distal monolayers (D. Siegel, unpublished calculations).

If traces of an apolar oil are dissolved in the bilayers, the interstice energy of the TMC would be removed. In this case, the "interfacial tension" of the inner sides of the distal monolayers would still drive dimpling of the distal monolayers, and the TMC would form. It would then continue to expand radially, as depicted in Fig. 10. The maximum stress on the distal monolayer diaphragm occurs before radial expansion of the TMC (see Discussion), so rupture (fusion) is most likely at that point. If very large amounts of apolar oil were available, it could be argued that the distal monolayers might remain planar during radial expansion of the *cis* monolayers of the stalk, leaving a diaphragm of planar distal monolayers separated by oil in the center of the structure. If this diaphragm becomes large enough, it could develop spontaneous wave instabilities capable of rupturing the diaphragm. It can be shown (D. Siegel, unpublished calculations) that the diameter at which the instabilities could develop is on the order of 0.1 μm. This requires a volume of oil greater than the volume of the phospholipid bilayers comprising such a structure. Given that the equilibrium solubility of long-chain alkanes or other long-chain apolar oils in bilayers is typically only a few volume percent, it is unlikely that this much oil could be assembled on the time scale of radial expansion of the stalk.

The general procedure for calculating the geometric mean curvature energy of stalks, TMCs, and ILAs is as follows. For stalks, the curvature energy of the *cis* (apposed) monolayer part of the structure is given by equation A1 of Siegel (1993) (note the typographical error in this equation described above). As discussed in the next subsection, the *trans* (distal) monolayers above and below the curved *cis* monolayers of the stalk are assumed to be flat; this configuration yields the lowest stalk energy of the two investigated configurations (Fig. A1) when the average value of ϵ is nearly zero, which is presumed to be true in the L_α phase. Hence these regions make no contribution to the curvature energy. For TMCs, the *cis* (apposed) monolayer part is treated with equation A1 of Siegel (1993), the semitoroidal parts of the *trans* (distal) monolayers by the same equation (but with the sign changes indicated in Siegel (1993)), and each of the spherical dimples in the *trans* monolayers by the following:

$$2\pi(k_m/2)r_3^2(1-\cos\phi)[\{(2/r_3)-C_0\}^2-C_0^2], \quad \text{(A1)}$$

where r_3 is the radius of the partial sphere and ϕ is the angle subtended by the spherical segment, measured from the axis of the TMC (see figure 8 *D* of Siegel, 1993). The values of r_3 and ϕ are related by

$$\phi = \cos^{-1}\left[\frac{r_3 + h/2}{r + r_3 + h}\right], \quad \text{(A2)}$$

where h is the monolayer thickness. In practice, for a given value of C_0, the TMC energy is calculated for a range of r and r_3, and the value of r_3 that generates the lowest energy structure is used. The TMC energy is fairly insensitive to changes in r_3 near the minimal value. The curvature energy of the *cis* and *trans* monolayers of the ILA are computed with equation A1 of Siegel (1993), using the different signs as indicated.

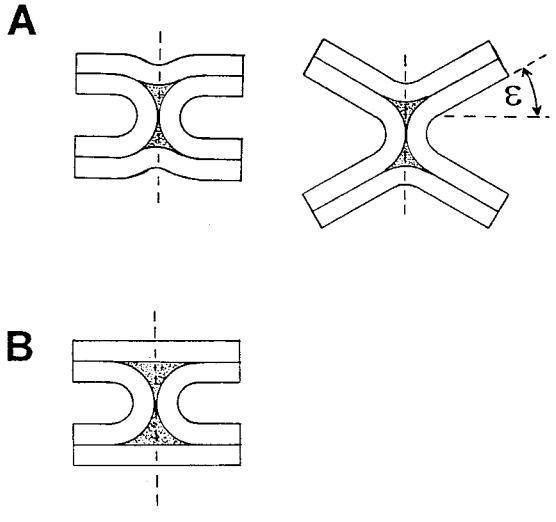

FIGURE A1 Different stalk geometries. All of the structures are cylindrically symmetrical around the dashed vertical axes. Hydrophobic interstices are indicated by stippled regions. (*A*) Stalks with dimpled distal (*trans*) monolayers overlying the hydrophobic interstices. The marginal angle ϵ is defined in the drawing at right. $\epsilon = 0$ for stalks existing between planar membranes. (*B*) Stalk with flat distal (*trans*) monolayers overlying the interstices. This is the lower energy configuration for $\epsilon = 0$.

Interstice energy calculations

The energies of the linear interstices in the H_{II} phase can be calculated in terms of the equilibrium dimensions of the H_{II} phase and the curvature elastic modulus of the lipid system (Siegel, 1993). This approach has proved successful in reproducing the phase diagram of DOPE in water (Kozlov et al., 1994). The energy of linear interstices in TMCs (Fig. 1 *C*), which are like the linear interstices in the H_{II} phase, can be accurately estimated by the same equations. The interstice energy of TMCs is calculated by multiplying the circumference of the centroid of the interstice by the expression for the energy per unit length of interstice (equation 7 in Siegel, 1993). For TMC interstices, the value of r_3 is used for r_H in equation 7 of Siegel (1993), because r_3 is the radius of the monolayer segments bounding two of the three sides of the interstice. The radius of the centroid of the interstice is given by equation A3 of Siegel (1993).

The energy of interstices in non-linear geometries, like those of the stalk (Fig. A1), are more difficult to calculate. It is likely that interstice energies are sensitive to changes in interstice geometry. There does not appear to be an equilibrium structure with interstices with this geometry that can be used to estimate the interstice energies in a model-independent fashion, as for TMC interstices. Previously, the energy of stalk interstices was estimated by volume scaling to the energy of linear interstices (Siegel, 1993). However, the form of the equations for the energy of H_{II} interstices suggests that, for small departures from equilibrium dimensions, the energies scale as the surface area of the interstices. Moreover, one way to envision the origin of interstice energies is as an effective "surface tension" that exists at the interface of the lipid methyl group layers and the idealized vacuum inside the interstice. Therefore, in the present work the stalk interstice energies have been calculated by surface area-scaling the energies of linear interstices. This results in an effective "interstice surface tension," γ. An expression for this effective tension is derived by dividing the free energy per unit length of a linear interstice (g_{tsv}; Siegel, 1993) by the interstice perimeter in the plane of its cross section. Using the expression for g_{tsv} derived previously (equation 4 in Siegel, 1993), we obtain for γ

$$\gamma = \frac{g_{tsv}}{(\pi+2)(r_T + h/2)} = \frac{\pi k_m}{2(\pi+2)(r_T + h/2)r_T}. \quad \text{(A3)}$$

r_T is the equilibrium monolayer radius in the H_{II} phase at a temperature T, which we fix as T_H, and h is the monolayer thickness. The energies of stalk interstices are calculated by multiplying the surface area of the interstices by γ. Stalk interstice energies are lower when calculated using surface area scaling. In this work we have calculated stalk interstice energies via this method. Using the same values of k_m and r at $T = T_H$ used by Kozlov et al. (1994) and $h = 1.8$ nm (Siegel, 1993), γ has a value of 1.94 erg/cm^2, or $\sim 0.476\ k_BT$/nm^2 at room temperature.

The overall shape of the stalk affects the shape of the interstice. As in Siegel (1993), the radii of the interfaces around the stalk are all assumed to be equal to simplify calculations. This seems appropriate, given the crudity of our model of how the energy of the stalk interstice changes as a function of geometry. Stalks are characterized by a marginal angle ϵ (see Fig. A1 *A*), which reflects the extent to which the two apposed bilayers are puckered toward each other at the periphery of the stalk. ϵ is zero if the two apposed bilayers are parallel at the periphery of the stalk, and ϵ is positive if the bilayers are locally puckered toward each other. In Siegel (1993) all stalks were assumed to have interstices with the geometry shown in Fig. A1 *A*

("axially symmetric voids," here referred to as "dimpled interstices"). This type of interstice requires the *trans* monolayer above it to form a dimple, and also requires the bilayers at the margin of the stalk to bend, increasing the curvature energy of the intermediate (Siegel, 1993; Eq. A2). In the course of the present work, a second type of interstice geometry was investigated, shown in Fig. A1 *B*. In this geometry, the *trans* monolayer is flat, and the bilayers do not have to bend in the vicinity of the interstice, which lowers the curvature energy of the stalk. However, the volume and surface area of the hydrophobic interstice are much larger than for the dimpled interstice, so the interstice energy is higher. Simple geometric analysis yields the surface areas of the dimpled and flat-topped interstices:

$$\begin{aligned} &\text{Flat-topped interstice:} \quad \pi(r + h/2)^2(\pi - 1) \\ &\text{Dimpled interstice:} \quad 2\pi(r + h/2)^2[(\pi/3) + 1 - \sqrt{3}]. \end{aligned} \tag{A4}$$

Here, r is the radius of curvature of the monolayers surrounding the interstice. For the same values of r and h, the surface area of the flat-topped interstice is 3.4 times larger than that of the dimpled interstice, and the interstice energies should be in the same ratio.

Calculations show that the curvature energy differences between stalks with flat-topped and dimpled interstices are much larger than the differences in interstice energies. Therefore stalks with flat-topped interstices have much lower energies than stalks with dimpled interstices when ϵ is near 0°. The converse is true for large values of ϵ. It is likely that ϵ is close to 0° in a lamellar lattice undergoing lamellar/inverted phase transitions. Therefore, in this work the stalks are assumed to have flat-topped interstices (Fig. A1 *B*), and it is assumed that $\epsilon = 0$. However, local membrane deformations, which appose patches of bilayer interfaces and increase ϵ, would lower the energy of both stalks and TMCs and enhance the formation rate of both structures. It is possible that there is some stalk configuration with small values of ϵ and an interstice geometry intermediate between Figs. A1 *A* and A1 *B* that would have a lower energy.

APPENDIX 2: ESTIMATING THE EFFECTS OF GAUSSIAN CURVATURE AND CHAIN-PACKING ENERGIES ON THE TEMPERATURE RANGE OF ILA STABILITY

Effects of Gaussian curvature elastic energy on the temperature range for ILA formation

The total Gaussian curvature elastic energy for a structure composed of closed monolayers can be evaluated by determining the number of closed, orientable monolayer surfaces of each genus (Andersson et al., 1988). Formation of a stalk or TMC between two apposed liposomes reduces the total Gaussian curvature elastic energy of the system by $4\pi\kappa_G$, and formation of an ILA lowers the energy twice as much. To a first approximation, therefore, this contribution to the ILA energy is the reduction in total Gaussian curvature energy of the entire system. The number of lipids per ILA, n_{ILA}, is given by

$$n_{ILA} = [2\pi^2(2r + h)(r + R + h) - 4\pi\{(r + h)^2 + r^2\}]/a. \tag{A5}$$

The Gaussian curvature elastic contribution to the ILA energy per lipid is $8\pi\kappa_G/n_{ILA}$. No measurement of κ_G in pure phospholipid systems is available. However, this value has been estimated in monoglyceride (Chung and Caffrey, 1994a) and lauric acid/dilauroyl-PC systems (Templer et al., 1994). In these reports, κ_G is estimated to be between 3 and 5% of k_m. If we assume that $\kappa_G/k_m = 0.04$ applies in PE systems, we can estimate the size of this contribution to the ILA energy. (Furthermore, using this value of κ_G/k_m, the effect of Gaussian curvature would lower the total energies of stalks and TMCs by $\sim 4\pi\kappa_G = 5k_BT$.) When the Gaussian curvature elastic contribution (with $\kappa_G/k_m = 0.04$) is added, the high temperature limit for ILA stability increases by only ~3° over the temperature calculated using only mean geometric curvature energy.

The lower temperature limit for ILA formation is substantially affected by inclusion of Gaussian curvature elastic energy. This energy stabilizes ILAs and would reduce this onset temperature even further than estimated in the Results. It is already anticipated that ILAs can form as soon as the temperature increases past T_c, even if only mean curvature elastic energy contributions are considered, so the Gaussian curvature term does not change the predictions of the theory.

Effects of chain-packing energy on ILA array stability

To minimize curvature gradients along their surfaces, groups of ILAs may deform into geometries with shapes somewhat different from the circular toroidal shape assumed here. The bilayer midplanes may conform to an infinite periodic minimal surface of similar overall shape. This might also involve local changes in monolayer thickness, so that the monolayer midplanes could conform to planes of constant curvature (Anderson et al., 1988). Anderson et al. (1988) found that the average deviation in monolayer thickness from the average value over the unit cell of Q_{II} phases could be as little as ~10% of the deviation over the H_{II} phase unit cell of the same lipids. It is expected that, in surfaces with low Gaussian curvature per unit area like ILAs, the deformations will be even more minor. We further assume that the chain-packing energy is linear in the root mean square deviation in local monolayer thickness, and that the average thickness is the "relaxed" value. Therefore, as a very rough indication of the contribution of chain-packing energies in ILAs and Q_{II} phases, it is assumed that the chain-packing energy per lipid in these geometries is 5% of the average interstice energy per lipid in the H_{II} phase. The chain-packing energy contribution to ILA energy is

$$\frac{a g_{tsv}(0.05)}{\pi r_H n_{ILA}}, \tag{A6}$$

where g_{tsv} is given by equation 4 of Siegel (1993). The combination of geometric mean curvature elastic and chain-packing energies is plotted in Fig. 4 (*open circles*). The inclusion of chain-packing energy destabilizes ILAs but decreases the upper limit of ILA array existence by only ~5° below the geometric mean curvature value. The small size of the effect is due to the fact that the slope of the H_{II} free energy plot is much greater than the slopes of the ILA free energy plots. However, chain-packing energy drastically increases the lower temperature limit for ILA array formation. It can be shown that inclusion of the chain packing energy assumed here is sufficient to increase the lower temperature limit to ~40 K below T_H. This is due to the small slope of the ILA free energy plots versus temperature (*left-hand side* of Fig. 4).

This work was supported in part by the National Institutes of Health (GM56969) and the Petroleum Research Fund (30537-AC7).

REFERENCES

Anderson, D. M., S. M. Gruner, and S. Leibler. 1988. Geometrical aspects of the frustration in the cubic phases of lyotropic liquid crystals. *Proc. Natl. Acad. Sci. USA.* 85:5364–5368.

Andersson, S., S. T. Hyde, K. Larsson, and S. Lidin. 1988. Minimal surfaces and structures: from inorganic and metal crystals to cell membranes and biopolymers. *Chem. Rev.* 88:221–242.

Basáñez, G., F. M. Goñi, and A. Alonso. 1998. Effect of single chain lipids on phospholipase C-promoted vesicle fusion. A test for the stalk hypothesis of membrane fusion. *Biochemistry.* 37:3901–3908.

Benedicto, A., and D. F. O'Brien. 1997. Bicontinuous cubic morphologies in block copolymers and amphiphile/water systems. Mathematical description through the minimal surfaces. *Macromolecules.* 30:3395–3402.

Briggs, J., and M. Caffrey. 1994. The temperature-composition phase diagram of monomyristolein in water: equilibrium and metastability aspects. *Biophys. J.* 66:573–587.

Caffrey, M. 1985. Kinetics and mechanism of the lamellar gel/lamellar liquid crystal and lamellar/inverted hexagonal phase transition in phosphatidylethanolamine: a real-time x-ray diffraction study using synchrotron radiation. *Biochemistry.* 24:4826–4844.

Caffrey, M. 1987. Kinetics and mechanism of transitions involving the lamellar, cubic, inverted hexagonal, and fluid isotropic phases of hydrated monoacylglycerides monitored by time-resolved x-ray diffraction. *Biochemistry.* 26:6349–6363.

Caffrey, M., R. L. Magin, B. Hummel, and J. Zhang. 1990. Kinetics of the lamellar and hexagonal phase transitions in phosphatidylethanolamine. Time-resolved x-ray diffraction study using a microwave-induced temperature jump. *Biophys. J.* 58:21–29.

Chen, Z., and R. P. Rand. 1997. The influence of cholesterol on phospholipid membrane curvature and bending elasticity. *Biophys. J.* 73: 267–276.

Chernomordik, L., A. Chanturiya, J. Green, and J. Zimmerberg. 1995a. The hemifusion intermediate and its conversion to complete fusion: regulation by membrane composition. *Biophys. J.* (in press).

Chernomordik, L. V., M. M. Kozlov, G. B. Melikyan, I. G. Abidor, V. S. Markin, and Yu. A. Chizmadzhev.1985. The shape of lipid molecules and monolayer membrane fusion. *Biochim. Biophys. Acta.* 812: 643–655.

Chernomordik, L., M. M. Kozlov, and J. Zimmerberg. 1995b. Lipids in biological membrane fusion. *J. Membr. Biol.* 146:1–14.

Chernomordik, L. V., G. B. Melikyan, and Yu. A. Chizmadzhev. 1987. Biomembrane fusion: a new concept derived from model studies using two interacting planar lipid bilayers. *Biochim. Biophys. Acta.* 906: 309–352.

Chernomordik, L., and J. Zimmerberg. 1995. Bending membranes to the task: structural intermediates in bilayer fusion. *Curr. Opin. Struct. Biol.* 5:541–547.

Chizmadzhev, Y. A., F. S. Cohen, A. Shcherbakov, and J. Zimmerberg. 1995. Membrane mechanics can account for fusion pore dilation in stages. *Biophys. J.* (in press).

Chung, H., and M. Caffrey. 1994a. The curvature elastic energy function of the lipid-water cubic mesophase. *Nature.* 368:224–226.

Chung, H., and M. Caffrey. 1994b. The neutral area surface of the cubic mesophase: location and properties. *Biophys. J.* 66:377–381.

Colotto, A., and R. M. Epand. 1997. Structural study of the relationship between the rate of membrane fusion and the ability of the fusion peptide of influenza virus to perturb bilayers. *Biochemistry.* 36:7644–7651.

Colotto, A., I. Martin, J.-M. Ruysschaert, A. Sen, S. W. Hui, and R. M. Epand. 1996. Structural study of the interaction between the SIV fusion peptide and model membranes. *Biochemistry.* 35:980–989.

Cullis, P. R., P. W. M. van Dijck, B. de Kruijff, and J. de Gier. 1978. Effects of cholesterol on the properties of equimolar mixtures of synthetic phosphatidylethanolamine and phosphatidylcholine. *Biochim. Biophys. Acta.* 513:21–30.

Ellens, H., J. Bentz, and F. C. Szoka. 1986. Fusion of phosphatidylethanolamine liposomes and the mechanism of the L_α-H_{II} phase transition. *Biochemistry.* 25:4141–4147.

Ellens, H., D. P. Siegel, D. Alford, P. L. Yeagle, L. Boni, L. J. Lis, P. J. Quinn, and J. Bentz. 1989. Membrane fusion and inverted phases. *Biochemistry.* 28:3692–3703.

Epand, R. M. 1985. High sensitivity differential scanning calorimetry of the bilayer to hexagonal phase transitions of diacylphosphatidylethanolamines. *Chem. Phys. Lipids.* 36:387–393.

Epand, R. M. 1990. Hydrogen bonding and the thermotropic transitions of phosphatidylethanolamines. *Chem. Phys. Lipids.* 52:227–230.

Epand, R. M., and C. T. Lemay. 1993. Lipid concentration affects the kinetic stability of dielaidoylphosphatidylethanolamine bilayers. *Chem. Phys. Lipids.* 66:181–187.

Erramilli, S., F. Osterberg, S. M. Gruner, M. W. Tate, and M. Kriechbaum. 1995. Time-resolved x-ray studies on pressure-jump induced topological transitions in biological membranes. *SPIE Proc.* 2521:188–196.

Evans, E., and D. Needham. 1986. Giant vesicle bilayers composed of lipids, cholesterol and peptides. *Faraday Discuss. Chem. Soc.* 81: 267–280.

Evans, E., and D. Needham. 1987. Physical properties of surfactant bilayer membranes: thermal transitions, elasticity, rigidity, cohesion, and colloidal interactions. *J. Phys. Chem.* 91:4219–4228.

Fournier, J. B. 1996. Nontopological saddle-splay and curvature instabilities from anisotropic membrane inclusions. *Phys. Rev. Lett.* 76: 4436–4439.

Frederik, P. M., K. N. J. Burger, M. C. A. Stuart, and A. J. Verkelij. 1991. Lipid polymorphism as observed by cryo-electron microscopy. *Biochim. Biophys. Acta.* 1062:133–141.

Gagné, J., L. Stamatatos, T. Diacovo, S. W. Hui, P. Yeagle, and J. Silvius. 1985. Physical properties and surface interactions of bilayer membranes containing N-methylated phosphatidylethanolamines. *Biochemistry.* 24: 4400–4408.

Gruner, S. M. 1990. Stability of lyotropic phases with curved interfaces. *J. Phys. Chem.* 93:7562–7570.

Gruner, S. M., M. W. Tate, G. L. Kirk, P. T. C. So, D. C. Turner, D. T. Keane, C. P. S. Tilcock, and P. R. Cullis. 1988. X-ray diffraction study of the polymorphic behavior of N-methylated dioleoylphosphatidylethanolamine. *Biochemistry.* 27:2853–2866.

Helfrich, W. 1973. Elastic properties of lipid bilayers: theory and possible experiments. *Z. Naturforsch. Sect. C Biosci.* 28C:693–703.

Hui, S. W., and T. P. Stewart. 1981. "Lipidic particles" are intermembrane attachment sites. *Nature.* 287:166–167.

Hui, S. W., T. P. Stewart, and L. T. Boni. 1982. Membrane fusion through point defects in bilayers. *Science.* 212:921–923.

Hui, S. W., T. P. Stewart, and L. T. Boni. 1983. The nature of lipidic particles and their roles in polymorphic transitions. *Chem. Phys. Lipids.* 33:113–116.

Keller, S. L., S. M. Bezrukov, S. M. Gruner, M. W. Tate, I. Vodyanov, and V. A. Parsegian. 1993. Probability of alamethicin conductance states varies with nonlamellar tendency of bilayer phospholipids. *Biophys. J.* 65:23–27.

Keller, S. L., S. M. Gruner, and K. Gawrisch. 1996. Small concentrations of alamethicin induce a cubic phase in bulk phosphatidylethanolamine mixtures. *Biochim. Biophys. Acta.* 1278:241–246.

Kirk, G. L., and S. M. Gruner. 1985. Lyotropic effects of alkanes and headgroup composition on the L_α/H_{II} lipid liquid crystalline phase transition: hydrocarbon packing vs. intrinsic curvature. *J. Physiol. (Paris).* 46:761–769.

Kozlov, M. M., S. L. Leikin, L. V. Chernomordik, V. S. Markin, and Yu. A. Chizmadzhev. 1989. Stalk mechanism of membrane fusion. Intermixing of aqueous contents. *Eur. Biophys. J.* 17:121–129.

Kozlov, M. M., S. Leikin, and R. P. Rand. 1994. Bending, hydration and interstitial energies quantitatively account for the hexagonal-lamellar-hexagonal reentrant phase transition in dioleoylphosphatidylethanolamine. *Biophys. J.* 67:1603–1611.

Kozlov, M. M., and M. Winterhalter. 1991a. Elastic moduli for strongly curved monolayers. Position of the neutral surface. *J. Phys. II (France).* 1:1077–1084.

Kozlov, M. M., and M. Winterhalter. 1991b. Elastic moduli and neutral surface for strongly curved monolayers. Analysis of experimental results. *J. Phys. II (France).* 1:1085–1100.

Kriechbaum, M., G. Rapp, J. Hendrix, and P. Laggner. 1989. Millisecond time-resolved x-ray diffraction on liquid-crystalline phase transitions using infrared laser T-jump technique and synchrotron radiation. *Rev. Sci. Instrum.* 60:2541–2544.

Laggner, P., and M. Kriechbaum. 1991. Phospholipid phase transitions: kinetics and structural mechanisms. *Chem. Phys. Lipids.* 57:121–145.

Laggner, P., M. Kriechbaum, and G. Rapp. 1991. Structural intermediates in phospholipid phase transitions. *J. Appl. Crystallogr.* 24:836–842.

Leikin, S. L., M. M. Kozlov, L. V. Chernomordik, V. S. Markin, and Yu. A. Chizmadzhev. 1987. Membrane fusion: overcoming of the hydration barrier and local restructuring. *J. Theor. Biol.* 129:411–425.

Leikin, S., M. M. Kozlov, N. L. Fuller, and R. P. Rand. 1996. Measured effects of diacylglycerol on structural and elastic properties of phospholipid membranes. *Biophys. J.* 71:2623–2632.

Leventis, R., N. Fuller, R. P. Rand, P. L. Yeagle, A. Sen, M. J. Zuckermann, and J. R. Silvius. 1991. Molecular organization and stability of hydrated dispersions of headgroup-modified phosphatidylethanolamine analogs. *Biochemistry.* 30:7212–7219.

Lewis, R. A. H., D. A. Mannock, R. N. McElhaney, D. C. Turner, and S. M. Gruner. 1989. Effect of fatty acid chain length and structure on the lamellar gel to liquid crystalline and lamellar to reversed hexagonal phase transitions of aqueous phosphatidylethanolamine dispersions. *Biochemistry.* 28:541–548.

Lewis, R. N. A. H., R. N. McElhaney, P. E. Harper, D. C. Turner, and S. M. Gruner. 1994. Studies of the thermotropic phase behavior of phosphatidylcholines containing 2-alkyl substituted fatty acyl chains: a new class of phosphatidylcholines forming inverted nonlamellar phases. *Biophys. J.* 66:1088–1103.

Lindblom, G., and L. Rilfors. 1989. Cubic phases and isotropic structures formed by lipids—possible biological relevance. *Biochim. Biophys. Acta.* 988:221–256.

Longo, M. L., A. J. Waring, and D. A. Hammer. 1997. Interaction of influenza hemagglutinin fusion peptide with lipid bilayers: area expansion and permeation. *Biophys. J.* 73:1430–1439.

Mannock, D. A., R. N. A. H. Lewis, R. N. McElhaney, M. Akiyama, H. Yamada, D. C. Turner, and S. M. Gruner. 1992. Effect of chirality of the glycerol backbone on the bilayer and nonbilayer phase transitions in the diastereomers of di-dodecyl-β-D-glucopyranosyl glycerol. *Biophys. J.* 63:1355–1368.

Mannock, D. A., R. N. McElhaney, P. E. Harper, and S. M. Gruner. 1994. Differential scanning calorimetry and x-ray diffraction studies of the thermotropic phase behavior of the diastereomeric di-tetradecyl-β-D-galactosyl glycerols and their mixture. *Biophys. J.* 66:734–740.

Markin, V. S., M. M. Kozlov, and V. L. Borovjagin. 1984. On the theory of membrane fusion. The stalk mechanism. *Gen. Physiol. Biophys.* 5:361–377.

Marsh, D. 1990. Handbook of Lipid Bilayers. CRC Press, Boca Raton, FL. 151.

McIntosh, T. J., S. Advani, R. E. Burton, D. V. Zhelev, D. Needham, and S. A. Simon. 1995. Experimental tests for protrusion and undulation pressures in phospholipid bilayers. *Biochemistry.* 34:8520–8532.

McIntosh, T. J., and S. A. Simon. 1986. Area per molecule and distribution of water in fully hydrated dilauroylphosphatidylethanolamine bilayers. *Biochemistry.* 25:4948–4952.

McIntosh, T. J., and S. A. Simon. 1996. Adhesion between phosphatidylethanolamine bilayers. *Langmuir.* 12:1622–1630.

Morein, S., E. Strandberg, J. A. Killian, S. Persson, G. Arvidson, R. E. Koeppe II, and G. Lindblom. 1997. Influence of membrane-spanning α-helical peptides on the phase behavior of the dioleoylphosphatidylcholine/water system. *Biophys. J.* 73:3078–3088.

Nanavati, C., V. S. Markin, A. F. Oberhauser, and J. M. Fernandez. 1992. The exocytotic pore modeled as a lipidic pore. *Biophys. J.* 63: 1118–1132.

Rand, R. P., N. L. Fuller, S. M. Gruner, and V. A. Parsegian. 1990. Membrane curvature, lipid segregation, and structural transitions for phospholipids under dual-solvent stress. *Biochemistry.* 29:76–87.

Rand, R. P., N. Fuller, V. A. Parsegian, and D. C. Rau. 1988. Variation in hydration forces between neutral phospholipid bilayers: evidence for hydration attraction. *Biochemistry.* 27:7711–7722.

Rand, R. P., T. S. Reese, and R. G. Miller. 1981. Phospholipid bilayer deformations associated with interbilayer contact and fusion. *Nature.* 293:237–238.

Seddon, J. M. 1990. Structure of the inverted hexagonal (H_{II}) phase, and non-lamellar phase transitions in lipids. *Biochim. Biophys. Acta.* 1031: 1–69.

Shyamsunder, E., S. M. Gruner, M. W. Tate, D. C. Turner, P. T. C. So, and C. P. S. Tilcock. 1988. Observation of inverted cubic phase in hydrated dioleoylphosphatidylethanolamine membranes. *Biochemistry.* 27: 2332–2336.

Siegel, D. P. 1986a. Inverted micellar intermediates and the transitions between lamellar, inverted hexagonal, and cubic lipid phases. I. Mechanism of the L_α-to-H_{II} phase transition. *Biophys. J.* 49:1155–1170.

Siegel, D. P. 1986b. Inverted micellar intermediates and the transitions between lamellar, inverted hexagonal, and cubic lipid phases. II. Implications for membrane-membrane interactions and membrane fusion. *Biophys. J.* 49:1171–1183.

Siegel, D. P. 1986c. Inverted micellar intermediates and the transitions between lamellar, inverted hexagonal, and cubic lipid phases. III. Formation of isotropic and inverted cubic phases and fusion via intermediates in transitions between L_α and H_{II} phases. *Chem. Phys. Lipids.* 42:279–301.

Siegel, D. P. 1993. Energetics of intermediates in membrane fusion: comparison of stalk and inverted micellar intermediate structures. *Biophys. J.* 65:2124–2140.

Siegel, D. P., and J. L. Banschbach. 1990. Lamellar/inverted cubic (L_α/Q_{II}) phase transition in N-methylated dioleoylphosphatidylethanolamine. *Biochemistry.* 29:5975–5981.

Siegel, D. P., J. L. Banschbach, D. Alford, H. Ellens, L. J. Lis, P. J. Quinn, P. L. Yeagle, and J. Bentz. 1989a. Physiological levels of diacylglycerols in phospholipid membranes induce membrane fusion and stabilize inverted phases. *Biochemistry.* 28:3703–3709.

Siegel, D. P., J. Banschbach, and P. L. Yeagle. 1989b. Stabilization of H_{II} phases by low levels of diglycerides and alkanes: an NMR, calorimetric, and X-ray diffraction study. *Biochemistry.* 29:5975–5981.

Siegel, D. P., J. L. Burns, M. H. Chestnut, and Y. Talmon. 1989c. Intermediates in membrane fusion and bilayer/non-bilayer phase transitions imaged by time-resolved cryo-transmission electron microscopy. *Biophys. J.* 56:161–169.

Siegel, D. P., and R. M. Epand. 1997. The mechanism of lamellar-to-inverted hexagonal phase transitions in phosphatidylethanolamine: implications for membrane fusion mechanisms. *Biophys. J.* 73:3089–3111.

Siegel, D. P., W. J. Green, and Y. Talmon. 1994. The mechanism of lamellar-to-inverted hexagonal phase transitions: a study using temperature-jump cryo-electron microscopy. *Biophys. J.* 66:402–414.

Sjölund, M., G. Lindblom, L. Rilfors, and G. Avidson. 1987. Hydrophobic molecules in lecithin-water systems. I. Formation of reversed hexagonal phase at high and low water contents. *Biophys. J.* 52:145–153.

Small, D. M. 1986. The physical chemistry of lipids. *In* The Handbook of Lipid Research, Vol. 4. D. J. Hanahan, series editor. Plenum Press, New York.

Tate, M. W., E. F. Eikenberry, D. C. Turner, E. Shyamsunder, and S. M. Gruner. 1991. Nonbilayer phases of membrane lipids. *Chem. Phys. Lipids.* 57:147–164.

Tate, M. W., and S. M. Gruner. 1987. Lipid polymorphism of dioleoylphosphatidylethanolamine and saturated and monounsaturated phosphatidylcholines of various chain lengths. *Biochemistry.* 26: 231–236.

Tate, M. W., and S. M. Gruner. 1989. Temperature dependence of the structural dimensions of the inverted hexagonal (H_{II}) phase of phosphatidylethanolamine-containing membranes. *Biochemistry.* 28:4245–4253.

Tate, M. W., E. Shyamsunder, S. M. Gruner, and K. L. D'Amico. 1992. Kinetics of the lamellar-to-inverted hexagonal phase transition determined by time-resolved x-ray diffraction. *Biochemistry.* 31:1081–1092.

Templer, R. H. 1995. On the area neutral surface of inverse bicontinuous cubic phases of lyotropic liquid crystals. *Langmuir.* 11:334–340.

Templer, R. H., J. M. Seddon, and N. A. Warrender. 1994. Measuring the elastic parameters for inverse bicontinuous cubic phases. *Biophys. Chem.* 49:1–12.

Tenchov, B., R. Koynova, and G. Rapp. 1998. Accelerated formation of cubic phases in phosphatidylethanolamine dispersions. *Biophys. J.* 75: 853–866.

Thomas, E. L., D. M. Anderson, C. S. Henkee, and D. Hoffman. 1988. Periodic area-minimizing surfaces in block copolymers. *Nature.* 334: 598–601.

Veiro, J. A., R. G. Khalifah, and E. S. Rowe. 1990. ^{31}P nuclear magnetic resonance studies of the appearance of an isotropic component in dielaidoylphosphatidylethanolamine. *Biophys. J.* 57:637–641.

Verkleij, A. J. 1984. Lipidic intramembranous particles. *Biochim. Biophys. Acta.* 779:43–63.

Verkleij, A. J., C. Mombers, W. J. Gerritsen, L. Leunissen-Bijvelt, and P. R. Cullis. 1978. Fusion of phospholipid vesicles in association with the appearance of lipidic particles as visualized by freeze-fracturing. *Biochim. Biophys. Acta.* 555:358–361.

Verkleij, A. J., C. Mombers, J. Lenissen-Bijvelt, and P. H. J. Th. Ververgaert. 1979. Lipidic intramembranous particles. *Nature.* 279:162–163.